# DEVELOPMENT OF A COMPREHENSIVE ELECTRO-THERMAL BATTERY MODEL FOR ENERGY MANAGEMENT IN MICROGRID SYSTEMS

Attanayaka Mukaweti Sahabandu Mudiyanselage Harindya Shehani Attanayaka

188031H

Degree of Master of Science by Research

Department of Electrical Engineering

University of Moratuwa

Sri Lanka

November 2019

# DEVELOPMENT OF A COMPREHENSIVE ELECTRO-THERMAL BATTERY MODEL FOR ENERGY MANAGEMENT IN MICROGRID SYSTEMS

Attanayaka Mukaweti Sahabandu Mudiyanselage Harindya Shehani Attanayaka

188031H

Thesis submitted in fulfillment of the requirements for the degree of Master of Science by Research

Department of Electrical Engineering

University of Moratuwa

Sri Lanka

November 2019

**DECLARATION**

I declare that this is my own work and this thesis does not incorporate without acknowledgement any material previously submitted for a Degree or Diploma in any other University or institute of higher learning and to the best of my knowledge and belief it does not contain any material previously published or written by another person except where the acknowledgement is made in the text.

Also, I hereby grant to University of Moratuwa the non-exclusive right to reproduce and distribute my thesis, in whole or in part in print, electronic or other medium. I retain the right to use this content in whole or part in future works (such as articles or books).

Signature: Date:

The above candidate has carried out research for the Masters/MPhil/PhD thesis/ Dissertation under my supervision.

Signature of the supervisor: Date

**ABSTRACT**

Energy storage systems are frequently used to buffer the difference between intermittent renewable generations and energy demand in microgrids. Different energy storage options are possible but the battery energy storage is in high demand in due to its advantages such as relatively fast response, less environmental impact, and diversity of technology and ability of recycling, over the alternative options such as ultra-capacitors, pump storage and flywheels. But the operation of a Battery Energy Storage System (BESS) is affected by dynamics of charging/discharging current, internal temperature build up, extreme reaches of SOC level etc. Therefore a battery model that can represent dynamic and static load changes, thermal response and SOC is important to monitor and control the BESS for a longer life time, enhancing sustainability and reliability of the microgrid.

This thesis describes the development of a comprehensive electro-thermal model for li-ion batteries that can be used to investigate dynamic and static performances of a microgrid under real time operating conditions. The battery-model has the ability to self-update its parameters with the variation of core-temperature, and also to accommodate inherent hysteresis present on parameters between charging and discharging events. The developed model is presented as a block in MATLAB/Simulink for easier use by others. In parallel with that, the details of the development of a complete simulation platform of a microgrid is also described, which includes battery charging and discharging converter systems, bi-directional grid-end AC/DC converter system, wind energy input, solar PV energy input, load and closed loop control associated with converter systems. The battery model is simulated within the microgrid platform with a chosen energy management criteria. The results of the simulation are also presented and discussed.

*Keywords— Battery Energy Storage System; Dynamic modelling; Electro-thermal model; Energy Management System; Equivalent Circuit Models; Microgrids; State of Charge; Thermal behavior*

**ACKNOWLEDGEMENT**

Foremost, I am deeply indebted to my supervisor Professor J.P. Karunadasa and co-supervisor Professor K.T.M.U. Hemapala of the Department of Electrical Engineering, University of Moratuwa for their constant guidance, encouragement and support from the beginning to the end. It is my pleasure to acknowledge all the other academic staff members of Department of Electrical Engineering of the University of Moratuwa for their valuable suggestions, comments and assistance which were beneficial to achieve the project objectives.

I am grateful to the University of Moratuwa for the financial grants under Senate Research Committee (SRC) Grant scheme and the Faculty of Graduate Studies for the given administrative support to conduct the research.

I thank to the technical officers and other support staff of the Electrical Machines laboratory and the power system laboratory for the assistance they have given to perform laboratory experiments.

Moreover, I would like to extend my gratitude to my family for their encouragement, understanding and patience throughout my academic pursuit. Finally I am grateful to my colleagues and friends for showing interest in my work and giving constructive ideas towards the success of the research.

**TABLE OF CONTENT**

**LIST OF FIGURES**

**LIST OF TABLES**

**LIST OF ABBREVIATIONS**

ESS : Energy Storage System

DG : Distributed Generation

BESS : Battery Energy Storage System

SOC : State Of Charge

ECM : Equivalent Circuit Model

BMS : Battery Management System

EMS : Energy management

PNGV : Partnership for a New Generation Vehicle

## 1. INTRODUCTION

Microgrids and their enabling technologies, such as Renewable Energy Generations and Energy Storage Systems, play vital roles when it comes to sustainable and clean energy [1]. Among different Energy Storage Systems (ESS), Battery Energy Storage System (BESS) have received greater attention at present due to their high reliability, possibility of implementing in medium scale-units, dynamic local voltage support, low environmental impact and many other factors [2] [3]. But the implementation and operation of BESS are surrounded by several challenges, such unbalanced loading and single-phase distributed-generating units, short term loading by EV (Electric Vehicles) charges, load dynamics due to intermittency of renewable power sources, inherent thermal build up in BESS, possibility of wide range fluctuation of battery SOC (State Of Charge) level, variation of battery performance with battery temperature etc. Therefore, in order to investigate the influence of all such issues on BESS an accurate model is required for the battery itself and the microgrid as a whole [3].

### 1.1 Problem Statement

Several battery models have been developed to design and investigate performance of the systems of EVs and BESSs involving batteries, categorized as Equivalent Circuit models, electrochemical models, empirical model and data-driven models. These models have their own advantages and disadvantages but none of the models had considered the combined thermal and electrical dynamics, despite the fact that two are highly interrelated. In particular, the changes in core temperature affect the values of battery parameters which in turn influence the electrical response. Similarly, electrical responses lead to changes in the core temperature.

Other than the core temperature, the parametric hysteresis between charging and discharging processes influence the battery dynamics in real systems, where battery is subjected to frequent fluctuations between charging and discharging. Again, not a single model available currently had incorporated this hysteresis effects meaningfully in to battery models.

The motivation of this research is to develop an advanced battery model incorporating the electrical, thermal and hysteresis type dynamics in to one model. The biggest

challenge in this type of modelling is achieving computational efficiency while handling cross-effects among constituent sub-systems. This will be addressed partly by adopting battery-type specific test data in to the model to characterize the hysteresis. Such battery data is obtainable by offline testing of different types of batteries and having them in a library.

A model will be more useful if it is made available as a "battery block", compatible with commonly used relevant simulation tools, such as MATLAB/Simulink with explicit terminals for external interconnections. Then the instantaneous values of terminal voltage and currents are readily available and other outputs such as instantaneous values of battery SCO, core-temperature, surface-temperature etc. needs to be separate outputs of the model.

The battery model that will be required to investigate broader performance of a battery will have to focus on the following aspects.

- Fast charging and discharging due to heavy current
- Internal dynamics
- Variation of battery voltage with temperature
- Inherent hysteresis between Charging and discharging
- Maintaining the battery SOC within an acceptable range
- Variation of battery parameters and performance with temperature
- The influence of ambient temperature on battery performance
- The design cooling system

## 1.2 Project Objectives and Scope

The main objectives of the research are:

- To develop a comprehensive electro-thermal combined model for a battery bank and present the same as a standard component in MATLAB/Simulink
- To develop a simulation test bed and investigate the performance of the battery model under different charging/discharging scenarios to validate the model.

The structure of the test bed for simulating the battery is shown in fig.1.1. This is a microgrid system that integrates Distributed Energy Sources (DES), diverse Energy Storage Systems (ESS), variable loads, and power electronic converting systems in a stable manner to ensure a reliable operation with grid connected mode under different renewable generation and load variation.

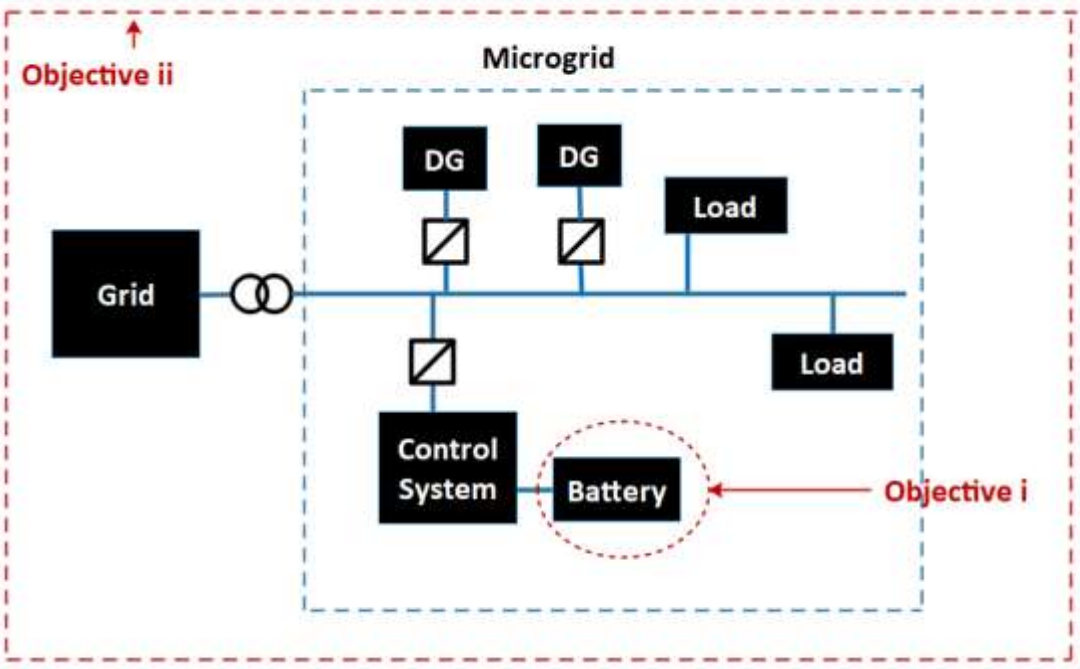


Figure 1.1: Scope of research

### 1.3 Energy Storage techniques

Distributed Generators (DG) in micro-grids involve renewable and non-renewable energy sources. Intermittent nature of renewable energy sources (Wind, Photo-Voltaic Systems, Biomass, tidal/wave energy, geothermal) demands suitable Energy Storage Systems (ESS) having fast response [2] [4]. Commonly, ESSs have several categories according to their technology, capacity, response time and capital cost. Among different ESS systems batteries, super-capacitors, hydrogen Energy storage and electrochemical capacitors can be considered as small scale ESSs [5].

Table 1.1: Characteristics of Energy Storage Systems [5]

| Energy Storage System | Key factors | Response time | Efficiency | Discharge time |
|---|---|---|---|---|
| Battery | • Long life time<br>• Minimal environmental impact<br>• Technical diversity | Seconds | 60% - 80% | min – 1 hour |
| Hydrogen Energy Storage (Fuel cell) | • Minimal environmental impact<br>• Production cost is higher (usage of platinum as the catalyst) | Seconds | 20% - 50% | Sec – 24 hours |
| Super-capacitors | • High power density<br>• High capital cost | Milliseconds | 84% - 94% | Milliseconds |
| Capacitors | • Technology development<br>✓ high-capacity capacitors with different electrodes | Milliseconds | | |

### 1.3.1 Battery Energy Storage System and lithium-ion batteries

Selection of a particular Energy Storage for a given application needs careful considerations, since different ESSs have different capacities, energy densities, response time, discharge time and efficiencies as listed in the table 1.1. Also, to balance the supply and demand in the long run (Energy Management) and the short run (Power quality management), the Energy Storage System must be adapted correctly [6]. In power quality management, the energy storage system must be able to respond to fluctuations very fast to preserve the power quality by maintaining the frequency and voltage level at the satisfactory range. In Energy Management, the Energy Storage Systems need to be inherited high capacities with high discharge time. Considering the above aspects, for microgrid application, the BESS are considered as the better ESS [7][8]. In particular, BESS have the following positive features.

- The possibility of implementation in medium-scale units (MW)

- Longer life cycles

  As lifespan depends on several factors including depth of discharge, discharge and charge cycles and environmental factors.
- Higher discharge time

  It is the maximum duration that ESS can discharge at rated power which depends on the available energy capacity, depth of discharge and operational conditions.
- Shorter response time
- Competitive cost
- High round-trip efficiency

  Key determinant of the cost-effectiveness of an ESS which for BESS is greater than 75%.
- Commercial availability of battery technology

  Availability of critical material (lithium-ion, Nickel Cadmium, Lead Acid, Sodium Sulfur)
- High discharge rate
- High re-charge rate

### 1.3.2 Lithium-ion battery technology

The diversity of different battery technologies is considerably broad. Table 1.2 shows the chemistry of lithium-ion, lead-acid, sodium-sulfur and nickel-cadmium type batteries [9] [10].

Table 1.2: Different battery chemistries [9]

| | |
|---|---|
| Lead Acid | |
| Nickel Electrode | Nickel Cadmium (NiCd) |
| | Nickel Metal Hydride (NiMH) |
| Sodium -Sulfur | |
| Lithium-ion | Lithium Cobalt Oxide (LCO) |
| | Lithium Manganese Oxide (LMO) |
| | Lithium Iron Phosphate (LFP) |

| | |
|---|---|
| | Lithium Nickel Cobalt Aluminum Oxide (NCA) |
| | Lithium Nickel Manganese Cobalt Oxide (NMC) |

Among different battery chemistries, lithium-ion can be considered as the most promising battery technology as it presents a considerable number of merit factors that prevails its own limitations as well as other batteries strengths. Even though lithium-ion batteries can be regarded as key potential component of sustainable energy management, achieving the goal must be accomplished by establishing policies, practices and decisions.

Table 1.3 shows the merits and demerits of lithium-ion battery technology [11].

Table 1.3: Advantages and disadvantages of li-ion battery [11]

| | |
|---|---|
| Merits | Remarkable specific power and energy with high load capacity power cells |
| | High calendar and cycle lives |
| | Excellent round-trip efficiency |
| | High reliability |
| | Relatively low operational and maintenance requirements |
| | Wide range of operating temperature |
| | Technological diversity with various battery chemistries and low environmental |
| | Negligible self-discharging |
| | Relatively fast charging schemes |
| | Low internal resistance |
| Demerits | Requirement of advanced BMS |
| | High initial cost |
| | Hazardous situations due to thermal runaways (safety issues) |

Li-ion battery contains four components anode, cathode separator and electrolyte. Generally, lithium-ion batteries are specified according to the cathode material, which determines the key properties of the battery. For commercial purposes several lithium-ion metal oxides are adapted along with li-cobalt oxide (LCO), li-ion

Phosphate (LFP), li nickel manganese cobalt oxide (NMC), li-manganese oxide (LMO) and li-titanium oxide (LiTiO). Table 1.4 shows details of the components of li-ion battery and table 1.5 shows the chemistries of different li-ion batteries.

Table 1.4: Components of li-ion battery [11]

| | |
|---|---|
| Cathode | LCO, LFP, NMC, LMO (lithium metal oxide) |
| Anode | Graphite |
| Electrolyte | A solation of lithium salt and organic solvent<br>Lithium salt :<br>• Lithiumperchlorate ($LiClO_4$)<br>• Lithium-hexafluorophosphate ($LiPF_6$)<br>• Lithium-hexafluoroarsenate ($LiAsF_6$)<br>• Lithium tetrafluoroborate ($LiBF_4$)<br>Organic solvent<br>• Ethyl-methylcarbonate ($C_4H_8O_3$)<br>• Diethylcarbonate ($C_5H_{10}O_3$)<br>• Ethylene-carbonate ($C_3H_4O_3$) |
| Separator | Polyethylene $(C_2H_4)_n$, Polypropylene $(C_3H_6)_n$ |

Table 1.5: Characteristics of different li-ion battery chemistries [11]

| | **Strengths** | **Shortcomings** |
|---|---|---|
| LCO | • High specific capacity and volumetric capacity<br>• self-discharge is low | • High cost (limited availability of Cobalt)<br>• Low thermal stability (thermal runways)<br>• Limited life span |
| LFP | • Wide SOC range<br>• High power capability<br>• High current rating<br>• Long life cycle<br>• Wide temperature range | • Low specific energy<br>• Lower electrical and ionic conductivity<br>• Higher self-discharge than other batteries |
| NMC | • High specific energy<br>• Acceptable cycling efficiency | • Low specific energy |

| | | |
|---|---|---|
| | • Lower cost (reduction on Cobalt) | |
| LMO | • Acceptable structural stability<br>• Higher thermal stability<br>• Eco-friendly materials | • Limited capacity<br>• Limited calendar and cycle life<br>• Low energy density |

### 1.4 Battery dynamic modelling

Most of the available battery models offer only the voltage and current responses at constant charging/discharging current, but the dynamic behavior due to fast varying charging/discharging current is not considered, due to the increases in complexity and the associated high computational cost [12]. Compromise between the model complexity and accuracy is an important factor when it comes to dynamic modelling of batteries. Also heat generation within the battery and rise of core temperature influence the battery characteristics in particular the internal resistance, Open Circuit Voltage (OCV) and the State of Charge (SOC) of the battery. Therefore, thermal modelling needs to be an important part of the dynamic modelling of a battery [13].

### 1.5 Energy Management System (EMS)

Microgrid with ESSs can effectively utilize renewable energy sources to compensate the demand, through a good Energy management Strategy. Such a system can minimize network losses and also lower the dependency on central generation without compromising reliability and other environmental concerns. Energy Management System coordinates the time varying energy profiles of the renewables sources with the variable demand through the BESS. Therefore the Energy Management System appropriately operates the power electronic subsystems incorporated with the ESS and other components in microgrid [14] [15]. Another prime objective of the Energy management Strategy is to observe the battery thermal behavior (distribution of battery core temperature, surface temperature) and initiate actions to preserve the safety of the battery. Monitoring the variation of battery characteristics is also a task of EMS [16]. Therefore, the main objectives of the EMS can be given as follows.

- To meet the demand by utilizing energy sources efficiently and economically without lowering power quality and continuity.
- To preserve the SOC level of the battery within the designated range
- To allow the battery to charge and discharge preserving the maximum chargeable and dischargeable power limits.
- To monitor the core temperature and surface temperature variation of the battery and initiate necessary actions to safeguard the battery.
- To operate the power electronic converting systems embedded with the microgrid components to achieve the intended energy management actions.

### 1.6 Thesis outline

The structure of the thesis can be depicted as follows. Chapter 2 summarizes different battery models presented in the literature. As State of Charge (SOC) of a battery is a key factor that influences the battery parameters, the estimation methods of SOC are also summarized both qualitatively and quantitatively.

Chapter 3 presents the thermal behavior of lithium-ion batteries and the impacts of temperature on battery properties and, eventually on the Battery Management System (BMS) that regulates charging/discharging. Furthermore, heat management of battery packs which ultimately leads to the control of temperature is also discussed with various cooling mechanisms.

Chapter 4 presents the proposed comprehensive electro-thermal battery model which incorporates battery dynamics and thermal response with appropriate cross couplings between electrical and thermal sub systems. Additionally, the proposed battery model is developed as a standard circuit element in MATLAB/Simulink platform to ease its adoption by other users.

Chapter 5 presents the test micro-grid platform, having a common DC busbar to which renewable energy sources, grid link, BESS and loads are connected. The BESS comprises the battery-bank and a bidirectional DC-DC converter between the DC-bus and the battery-bank. The battery-bank is modelled with the new battery model. The bidirectional DC-DC converter is controlled in closed loop to deliver controlled charging and discharging current under the commands of the overall energy

management strategy. Grid-link comprises a bidirectional AC-DC converter between the DC-bus and the grid AC system. This bidirectional AC-DC converter is controlled in the closed loop to regulate the DC-bus voltage at the set value for all times by transferring power in either direction as appropriate. Details of all modellings and models are presented. Energy Management Criterion of the microgrid is also presented.

Chapter 6 presents simulation results and relevant discussion. In particular, the battery current, core-temperature, surface-temperature and SOC when the microgrid is on a typical daily load curve with typical renewable inputs are presented and discussed.

Chapter 7 gives the conclusion and other salient achievements in the research followed by recommendation for future improvements and limitations.

## 2. Dynamic Modelling of battery cell

Accuracy of battery-cell model predicting and reflecting battery performance on different loading, environmental and operational conditions is crucial for an effective design of a micro-grid system with BESS, targeting high level of reliability and power quality.

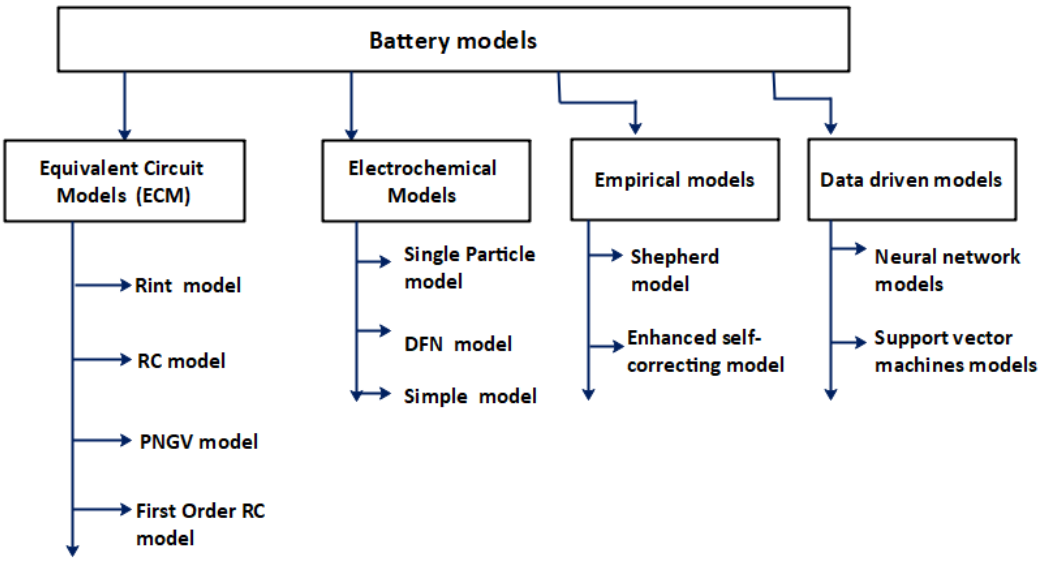


Figure 2.1: Classification of battery models [17][18][19]

Figure 2.1 illustrates classification of different battery models found in literature. Different models have different emphasis on key modelling features, namely nonlinear electrochemical process, dynamic response, heat generation, impact of temperature rise, Open Circuit Voltage (OCV) and polarization time constants. These models include Empirical models, physical models, Electrical Equivalent Circuit models (ECMs) and electrochemical models each having different levels of complexity, accuracy and physical interpretation for their suitability for dynamic modeling.

In order to express the chemical processes inside a battery, electrochemical models employ mathematical equations (Partial Differential Equations) and empirical data to derive the model coefficients [20]. On the contrary, the ECMs employ basic circuit elements of resistances, capacitances, and voltage sources to establish the relationship between the applied current and the battery terminal voltage [21].

## 2.1 Electrochemical models

Electrochemical models present possibly the most precise and comprehensive parallel of the complex process inside the battery. These models are obtained from concepts of electrochemistry, and are more accurate compared to the other modeling techniques, but the complexity and computation time are far greater. The frequently used model is the Single particle Model (SPM) which is a reduced electrochemical model.

The single-particle model (SPM) is modelled as spherical particle and it is assumed that lithium-ion accumulation in electrolyte is constant. This assumption leads to more accurate results at low current rates, but for higher current rates, the error is considerably large. Since it excludes the effect of temperature, the battery terminal voltage is only presented as a function of the applied current and boundary conditions [19] (which include li-ion concentration and charging/discharging current).The model has two linear diffusion Partial Differential Equations that describes the material diffusion in electrolyte. The output voltage map is determined using electrical potential, electrode thermodynamic properties as well as other kinetics equations [20].

## 2.2 Equivalent Circuit Models (ECM)

ECMs get the preference for accurate modelling of dynamics behavior at a reduced computational burden over the electrochemical models since the latter exhibits limitations, such as high complexity and inability to accurately represent dynamic behavior. ECMs are relatively simpler and widely employed in power system applications and Battery Management Systems. They simulate voltage-current behaviors of the battery bank and monitor the operation and control of the BMS. Accordingly, hazardous damages and disturbances in the BMS can be avoided with the application of properly implemented ECM. When it comes to selecting an accurate ECM, a great attention needs to be paid to strike a compromise between the complexity of the model and computational cost /time associated with the model

ECMs are divided into several sub models such as Rint model, RC model, PNGV model, first order RC model (Thevenin model) and the second order RC model (improved Thevenin model) as given in figure 2.2, 2.3, 2.4, 2.5 and 2.6 respectively. Amongst them the second order RC model adequately reflects the response to static and dynamic conditions.

### 2.2.1 Rint model

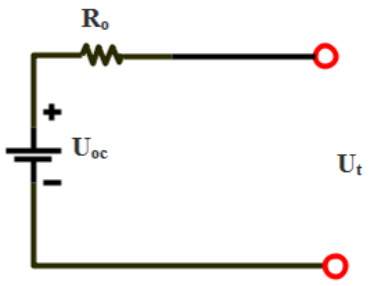


Figure 2.2: Rint model [21]

$R_o$ = internal resistance

$U_{oc}$ = Open Circuit Voltage

$V_t$ = Terminal voltage

I = Discharge current

The Rint model is the simplest among all ECMs and its computational burden is significantly low. But it fails to capture the fast charging/discharging phenomenon as it only represents the internal impedance by $R_o$. Equation (2.1) shows the dependency between the applied current and battery terminal voltage.

$$V_t = (U_{oc} - R_0 I) \qquad (2.1)$$

### 2.2.2 RC model

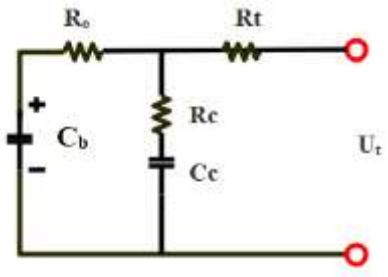


Figure 2.3: RC model [21]

$C_b$ = Battery capacitance

$R_t$ = End resistance

$R_c$ = Resistance due to surface effect

$C_c$ = Capacitance due to surface effect

$R_o$ = Internal resistance

Capacitance $C_c$, which is much smaller than $C_b$, accounts for the phenomenon of fast charging/discharging. The main drawback of RC model is that it has less ability to present the response to dynamics of charging/discharging current.

### 2.2.3 PNGV (Partnership for a New Generation Vehicle) model

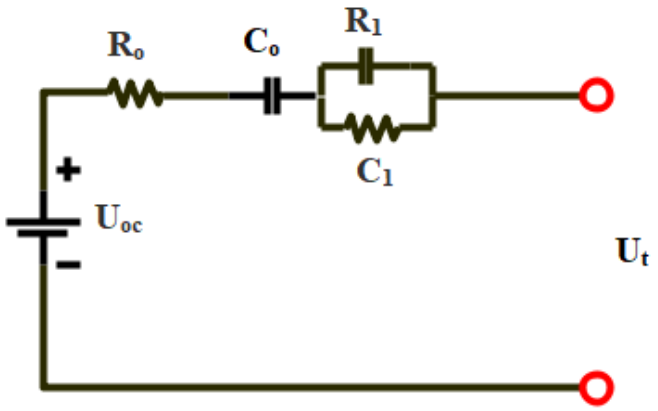


Figure 2.4: PNGV model [24]

$U_{oc}$ = Open Circuit Voltage

$R_o$ = Internal resistance

$R_1$ = Polarization resistance

$C_1$ = Polarization capacitance

$C_0$ = Bulk Capacitance

The PNGV model is more accurate than the RC model and Rint model [24]. $C_0$ accounts for the changes of the OCV of the battery. It captures the battery dynamic response to some extent.

### 2.2.4 First Order RC ECM (Thevenin model)

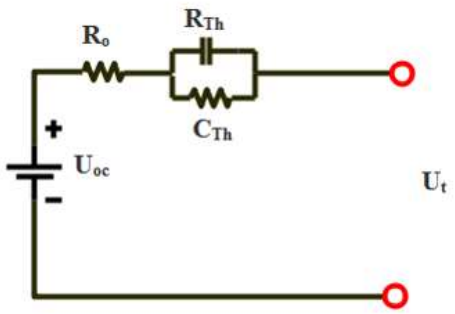


Figure 2.5: First Order RC ECM

$U_{oc} =$ Open Circuit Voltage

$R_o$ = Internal resistance

$R_{th}$ = Polarization resistance

$C_{th}$ = Polarization capacitance

The first order RC ECM is a good compromise between the accuracy and the complexity, in which RC branch reflects the relaxation effect due to charging/discharging processes. Even though it captures the dynamic behavior, the accuracy is still less than the PNGV model [22][23][25].

### 2.2.5 Second Order RC ECM (Improved Thevenin model)

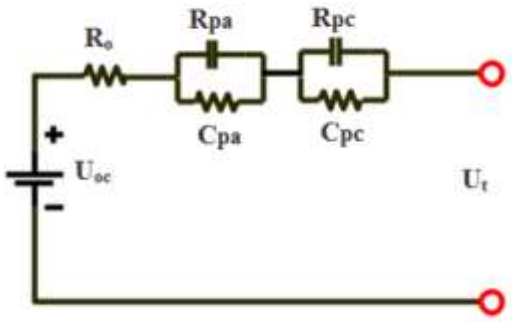


Figure 2.6: Second Order RC ECM

$U_{oc} =$ Open Circuit Voltage

$R_o$ = Internal resistance

$R_{pa}$ = Activation polarization resistance

$C_{pa}$ = Activation polarization capacitance

$R_{pc}$ = Concentration polarization resistance

$C_{pc}$ = Concentration polarization Capacitance

### 2.3 Estimation methods of Battery State of Charge (SOC)

The SOC of a battery is expressed as the ratio between its current capacity *Q(t)* (see equation (2.2)) and the nominal capacity $Q_n$ which demonstrates the maximum amount of charge which can be accumulated in the battery [26].

$$SOC(t) = \frac{Q(t)}{Q_n} \qquad (2.2)$$

SOC is information on battery performance and remaining life, instrumental for effective management and a guideline to the maximum usage of battery's power [27]. With a precise estimation of SOC it is possible to regulate the battery over-discharging and over-charging and thereby to uphold battery life and avoid explosion, flame, accelerated aging and structural damages to batteries [28]. Also, accurate SOC indication is a convenience to the user to ensure battery's efficiency, safety, and longevity. Thus, an accurate estimation of SOC is a fundamental requirement for a proper use a battery, minimizing failures due to thermal runaways and regulating the cell balancing.

Most of the SOC estimation techniques require precise analysis of either the battery chemical composition (type of electrolyte and its operating conditions) or cell variables (voltage, current). So, they are only suitable for laboratory environments rather than real world applications. One SOC estimation method that may be more convenient or applicable for a particular application may not be appropriate to another application [29]. Furthermore the SOC of a battery is not a state that can be measured directly but estimated through other parameters including current, voltage temperature and sometimes the battery history.

The algorithm of SOC estimation is generally programmed in the Battery Management System (BMS). The latter controls the energy flow in the battery pack

according to voltage of single cell, temperature, state of charge and state of health. The main function of BMS is to provide a safe operating condition for the battery system, and to prevent hazardous situations [30][31]. Even though the estimation of battery SOC is an essential function of BMS, its accuracy and online estimation is challengeable due to non-linear complex electrochemical process in the battery.

### 2.3.1 Direct Measurement Methods

In these methods, to estimate SOC, physical measurements of voltage and impedance of the battery are employed [33]. The frequently used direct measurement methods are OCV method, terminal voltage method, impedance method and impedance spectroscopy method.

#### 2.3.1.1. OCV Method

OCV is defined as the thermodynamic potential of the battery under no load condition. And it has a non-linear relationship with SOC for lithium ion batteries [34]. So, by knowing the OCV-SOC relationship, it is possible to find SOC in terms of the measured value of OCV. The OCV is usually acquired through offline OCV assessments at definite temperatures and aging levels.

Even though the OCV method is the simplest method, it requires a rest time to estimate the SOC and hence it is difficulty to apply in real world scenarios.

Furthermore different batteries have distinct OCV–SOC relationships and therefore an unacceptable error can occur if a different OCV–SOC data is used [35]. Generally, the dependency of OCV on SOC is estimated by calculating the OCV at each SOC stage. Even for the batteries of same chemistries and structures, the OCV-SOC curves can be different for different battery capacities. Moreover, obtaining of OCV-SOC curve for a given battery is a considerably time-consuming process [35].

OCV hysteresis can significantly influence SOC estimation. Hysteresis can be defined as the dissimilarity between the OCV on charging process and the OCV on discharging process [36]. Therefore it can be stated that the information of OCV alone is not sufficient to determine the SOC and the history of charge-discharge is also required.

Furthermore the hysteresis characteristics differ with the type of electrodes in li-ion batteries. To establish the impact of hysteresis, OCV should be measured for different SOC against charging and discharging, separately. The OCV-SOC relationship is then implemented either as an analytical expression or look-up table, the former being attractive in terms of data processing efficiency [37].

#### 2.3.1.2. Terminal voltage method

This is an extension of the OCV method, where OCV is computed from measured values of terminal voltage and battery current (knowing the internal resistance) [33]. It can be stated that only a minimal emphasis has been given in literature to determine SOC using terminal voltage method.

#### 2.3.1.3. Impedance method

AC impedance of a battery depends on the AC frequency and the SOC. The change of the impedance with frequency is greater when the SOC is lower and negligible when the SOC is higher. In the impedance-method, the SOC is estimated in terms of the measured impedance over some range of frequency. Impedance is measured by injecting a current of the desired frequency and measuring the voltage arising between the battery terminals.

#### 2.3.1.4. Impedance Spectroscopy method

Electrochemical Impedance Spectroscopy (EIS) method brings significant information about the complex electrochemical processes occurring inside the battery. Even though there are many EIS methods of estimating SOC, the complexity of each is considerably high [38]. In one approach, an impedance model is constructed with EIS data as a Nyquist plot, where the measured impedance is plotted as the real part against the imaginary part. The Nyquist plot impedance spectra is parted into three section: low frequency, mid frequency and high frequency.

### 2.3.2 Book keeping Methods

The coulomb counting method and modified coulomb counting method fall under this category. The battery charging/discharging current is taken as the input to these methods. These methods allow adding several internal effects of the battery, such as capacity-loss and self-discharge in to SOC estimation [33]. Nominal battery capacity is also an input to the estimation.

#### 2.3.2.1. Coulomb Counting method

In the coulomb counting method (Ampere-hour method), the SOC estimation is done by cumulating the charge flowed in and out of the battery [39]. The accuracy of the coulomb counting method is affected by the accuracy of initial SOC estimation and measurement of the battery current (accuracy of current sensors). The coulomb counting method is convenient for batteries with high discharging and charging efficiencies and required long time monitoring. Even though the method is not applicable for real-time SOC estimation, it can be employed to verify accuracy of the results obtained by other estimation methods.

$$SOC(t) = SOC_0 - \frac{1}{C_{rated}} \int i(t)dt \qquad (2.3)$$

According to the equation (2.3), $SOC_0$ is the initial SOC value and *i(t)* is the current with a negative value at charge, $C_{rated}$ is rated capacity. The initial SOC value ($SOC_o$) can be obtained by OCV method. Even though the method is simple and inexpensive, there are several drawbacks as listed below [40].

- Since the coulomb counter is an open loop estimator, deviations due to the current measurement is added by the estimator. The cumulative error becomes larger, when the SOC estimator operates through a longer time period. Also, an incorrect result can be generated faster, when then current sensor has larger errors.
- When the battery ages in real time, the battery capacity varies, but the coulomb counter cannot detect or take measures for the issue. As a result, the estimation might not be accurate, if the real pattern of the battery estimation deviates from the expected pattern.
- The initial SOC should be estimated by the terminal voltage of the battery pack. So any error contained in the initial estimation method will be carried throughout the process and this method cannot detect or repair the initial error.

The Coulomb Counting method can be improved by considering the Coulombic efficiency (Ah) at different temperature and charge rates. According to the equation (2.4), Coulombic efficiency is expressed as the ratio between the amount of charges extracted during the discharging process and the amount of charges entered during the charging process or the ratio of the discharging capacity to the charging capacity [41].

$$\eta_{Ah} = \frac{Q_{discharge}}{Q_{charge}} \qquad (2.4)$$

Since $\eta_{Ah}$ depends on the current rate (discharge or charge) as mentioned above, an Equivalent Coulombic Efficiency (ECE) ($\eta_{eq}$) is developed including the discharge and charge Coulombic Efficiency. According to the equation (2.5), the modified Coulomb Counting equation can be depicted with $\eta_{eq}$ and $C_a$, representing the ECE and the currently available capacity, that differs from the rated capacity $C_{rated}$ due to temperature and age effect [42].

$$SOC(t) = SOC_0 - \frac{1}{C_a}\int \eta_{eq} i(t)dt \quad (2.5)$$

Among the different battery chemistries, li-ion batteries offer the highest Coulombic efficiency in the normal SOC region (exceeds 99%) [41]. But the estimation of Coulomb efficiency is difficult task as it requires highly accurate equipment.

### 2.3.3 Indirect measurement

The adaptive systems are consistent, because of their ability to deal with the nonlinearities of battery systems and show considerably excellent accuracy. Yet, in order to obtain good results from the adaptive systems, the specific information of battery characteristics or an accurate Equivalent Circuit Model (ECM) are required [43].

#### 2.3.3.1 Neural Network method

Neural Network is a model (subfield of artificial intelligence) that contains interrelated artificial neurons stimulated by biological neural networks to forecast output based on past data. Neural Network methods do not depend on electrical, physical, thermal or chemical model and need small time period to generate results compared to Extended Kalman Filter (EKF) [44]. Neural Network consists of inputs and outputs and is made of a several number of processing units named neurons interconnected with each other. The accuracy of Neural Network method depends on how far the network is trained. The training process is the most important phase.

The most two common network architectures to estimate the SOC are the nonlinear input-output (NIO) feed-forward network and nonlinear autoregressive with exogenous input (NARX) feed-back network. Figure 2.6 presents the structure of a feed-forward neural network. In order to represent the input variables and output variables, the neural network contains an input layer with nodes and output layer, respectively. Additionally there are one or more hidden layers to simulate the nonlinearity between the input variables and output variable and each adjacent layers are interconnected [45]. Only the output layer and the hidden layers are the processing layers with activation functions at each nodes. There are several types of activation functions such as logistic tanh-hyperbolic tangent and ReLu-rectified linear units. In

most scenarios hyperbolic tangent sigmoid function and the linear transfer function are used as functions of activating the hidden layer and the output layer, respectively. As there are no theoretical criteria when it comes to deciding the number of hidden layers and the neurons, it will be done using the expertise knowledge. In regarding to the SOC estimation, the neural network method determines the SOC direct from the terminal voltage and applied current without the mapping OCV-SOC. The following steps can be considered as the constructive approach to the neural network SOC estimation.

1. Initialization (determination of the dimensions of the input layer and the number of neurons in the hidden layer).
2. Train the neural network with input variables (current, voltage, temperature) and output variable (SOC).
3. Error calculation between the actual inputs and the estimated output
4. If the error is within the expected level searching is ended; otherwise repeat the step 2

There are several factors that affect the SOC. Input current, terminal voltage and temperature [46] can be considered as the most vital parameters; these three parameters are selected as the input to the network. The battery SOC value is the output. The number of neurons in the hidden layer is set in accordance the experience [46].

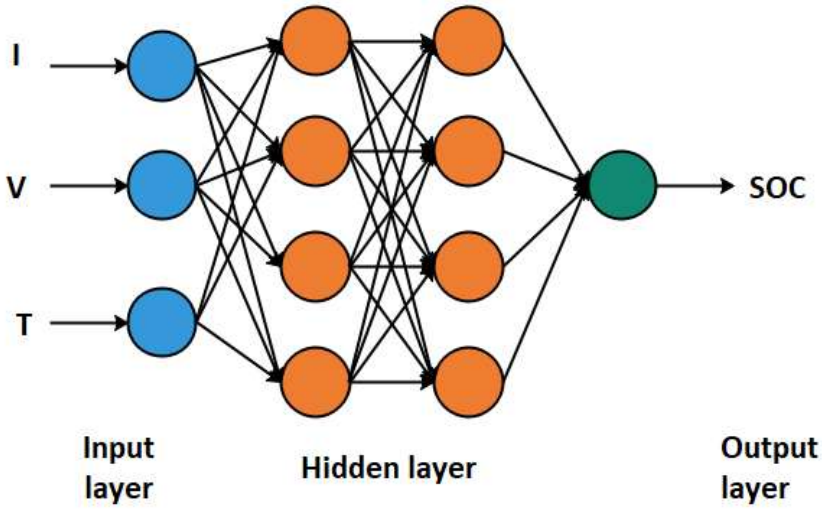


Figure 2.6: Predicting model for SOC based on neural network

#### 2.3.3.2 Kalman filter

Kalman filter (KF) is a recognized method, used to determine the inner state of dynamic linear system with an optimal estimating technique. Basically, KF is a recursive set of equations which has two steps: prediction step which predicts the system output, system state and error [47] and correction step which corrects the present state estimate based on the output value of the system [47]. The block diagram of Kalman filtering process is shown in figure 2.7. In order to design estimate SOC using Kalman filter, a battery state-space model is developed using the equivalent circuit model. Considering the system noise and observation noise, the discrete state-space model is developed. Since the battery OCV and SOC has a non-linear relationship and KF algorithm is only suitable for linear systems, a linearization method should be followed with an acceptable accuracy as a supplementary part. As a result of the linearization process, the discrete space-state model equation (output equation) is reduced to a less complex condition. The error between the measurable value and system state variable (ex: SOC) is calculated the KF using the output equation. Then the Kalman gain is adapted to update the system variables (SOC). Due to the highly nonlinear characteristics of battery system and unsuitable battery model inaccurate outputs can be generated in KF method.

Basically, input is the applied current, output is the terminal voltage, and SOC is placed as the hidden state [48]. Then the hidden state is estimated by one of KF, EKF, Unscented Kalman Filter (UKF) or Particle Filter (PF). In the EKF method, the Jacobian matrix must be constructed and if the system is highly nonlinear with non-Gaussian noise, the results may be generated with large errors [49]. But as an advantage, if there is an incorrect initial SOC value, the KF system can conquer it and could detect and represent cell aging.

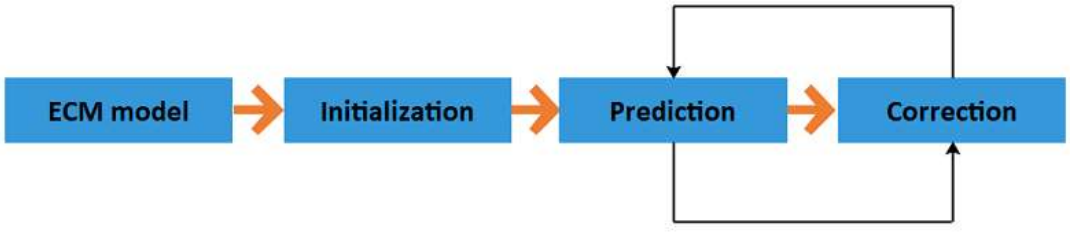


Figure 2.7: Kalman Filter Process

#### 2.3.3.3 Extended Kalman Filter

Extended Kalman Filter (EKF) is the improved version KF which is employed to determine the inner state of a nonlinear dynamic system using a state-space model [50]. Simply it predicts the future state of system based on the previous data [51]. When it comes to estimating SOC, it employs advanced battery models, therefore computation cost and time is relatively high.

The EKF consists of two equations. One equation consists of matrices constructed using the parameters of ECM, along with the system state matrices (SOC), measurable input matrices and non-measurable process noise [52]. The parameters will be identified performing standard test procedures. The second equation is the measurement equation which shows the output voltage in terms of system state vectors, measurable input matrices and measurement noise. Employing appropriate software tool (MATLAB Simulink) SOC can be estimated.

In some EKF methods, an inner filter is constructed to adjust the SOC and the battery model is adjusted by an outer filter [53]. According to the SOC and the cell model, the inner filter presents a corresponding voltage according to the input current. The SOC is adjusted by comparing the measured voltage and proposed voltage. Then, the system feedback is voltage and its output is SOC. After monitoring the applied current and voltage over a long period of time, the outer filter gradually modifies the parameters of the model. In this method, the cell aging and other lifetime effects are considered and modeled in real time. An advanced battery model should be established in order to achieve better results from the EKF method and the battery system must be treated as a nonlinear time-variant dynamic system [50]. Most common models are shepherd model, Unnewehr Model, Linear Model, Nernst Model, Thevenin model and RC Model [54]. The EKF algorithm not only can be used for online SOC estimation and track the battery state of charge parameter, but also can be utilized to estimate the parameter of the battery model [54].

#### 2.3.3.4 Unscented Kalman filter

Since SOC estimation of lithium-ion battery system inherits highly non-linear characteristics [55], it can produce large errors for EKF method, because it is a first or second order Taylor series expansion to estimate the nonlinear functions [54]. Apart from the above disadvantage, EKF must compute the Jacobian matrix and if the system consists of non-Gaussian noise, the produced results may not be at an acceptable level. So Unscented Kalman Filter (UKF) has been established to improve the accuracy of KF and EKF methods. Since the UKF deals with non-Gaussian noises as well and Jacobian matrix is not calculated, it is more suitable for SOC estimation [49].

In this method the battery's SOC is selected as a component of the state vector. The two sub models in the UKF methods are the process model and measurement model, which illustrate the relationship between the SOC and cell states such as, input current, voltage and temperature.

#### 2.3.3.5 Fuzzy logic

Fuzzy logic method can be used to model, non-linear and time-varying systems without the need for mathematical models or ECMs of a battery [56]. For the estimation of SOC using Fuzzy logic method, environmental temperature, applied current and battery terminal voltage are considered as the input variable balancing the complexity and accuracy well. The higher the number of input variables (dimensions of fuzzy controller), more accurate are the results. But when the dimension is higher, the rules of fuzzy control will be much complex to implement [57]. As the first step, Fuzzification is the mapping from the above input with fuzzy variables using membership functions. Membership functions can be triangular-shaped or trapezoidal-shaped functions considering the memory storage and efficiency. In the second step, the relationship between the input and output is described using rule based representation of expert knowledge [58]. The third step is the rationalizing mechanism that conducts inference procedure. Defuzzification is the third step that converts the modified control outputs into real valued outputs. The membership functions and rule sets are defined by generating as a result of neural network algorithm or an expert. To accurately forecast the SOC of the battery without considering the initial capacity using fuzzy logic model, a "training" data array are constructed [59].

In most fuzzy logic methods, the SOC value of the battery is predicted without the rated capacity or previous data of the discharge history of the cell and only by calculating the imaginary part of the impedance at a few selected frequencies [60].

In most scenarios, clustering algorithms are employed to construct input membership functions and rules. The output membership parameters are optimized using least square fit.

#### 2.3.3.6 Support Vector machines

Support Vector Machines (SVM) are a set of interconnected learning methods adopted for regression and classification that can be generally appropriate for any multi-variable function to a higher accuracy level [54] and have been effectively applied especially in highly nonlinear systems.

In order to estimate SOC using SVM regression model temperature, current measurement and voltage are considered nonlinear input variables [55]. Using a kernel function in the SOC estimation process, a training data set of the above input variable which covers the expected range of operation should be selected [33], [56],. Then the proposed SVM model is validated using the new data not used for training.

#### 2.3.3.7 Particle filter algorithm

Particle filter (PF) is an effective nonlinear filter technique that can obtain the particles and corresponding weight values through random sampling [62]. The principle is to represent the probability densities with a set of weighted particles [62]. The preciseness of the PF algorithm relies on the experimental data and the structure of the PF. In order to estimate SOC using PF algorithm method, it is necessary to establish a discrete state-space model which consists of state equation and observation equation [63]. The state equation is derived by the SOC definition which is expressed in the coulomb-counting method. The observation equation is obtained considering the terminal voltage of the second order RC equivalent circuit as the observed valued. The

parameters of the second order RC ECM is acquired through standard test procedures [64].

The collected data from charging process or discharging process data are stored as experimental data. Then to establish the state equation of the state-space model, the SOC estimation equation is discretized and considering the characteristics of collected data.

The particle filter algorithm has high accuracy for SOC estimation and the estimation error is comparatively small [65]. Using PF algorithm as an individual SOC estimation method, combination of PF and KF, PF and EKF, PF and EKF will improve the robustness of the KF algorithm while solving probability distribution function selection of PF algorithm [65].

### 2.3.4 Analyze of the SOC estimation methods

#### 2.3.4.1 Qualitative analysis

Considering the ability to represent dynamic response and less complexity of the model, the second order RC Equivalent Circuit Model can be considered as the most suitable model for microgrid environment (see figure 2.6)

Since the OCV in the second order ECM varies nonlinearly with SOC, when identifying the OCV, it is necessary to consider the battery SOC as an input to the simulation process [69]. So an appropriate SOC estimation method should be included for the modelling of BESS. Therefore it is important to identify a suitable SOC estimation approach to update the OCV (controllable voltage source) of the ECM. Also when selecting a method, the dynamic modelling of the battery must be preserved. The objective can be achieved by either adopting model-based SOC approach which calculates SOC and update OCV in the same procedure or adopting non-model based method to estimated SOC as an input to the ECM. The most frequently used ECM model-based SOC techniques are Kalman Filter methods such as EKF, UKF, CKF (Cubature Kalman Filter) and PF algorithm which consist of both estimator and battery model [70]. All other methods considered are non ECM-based methods which usually use physical parameters, with mathematical or artificial intelligence algorithms.

A very important aspect to be considered is the thermal behavior of li-ion battery and how it affects the operation of the BESS. The battery internal resistance and battery capacity are influenced by temperature distribution in terms of battery lifetime degradation or battery performance [92]. Furthermore round-trip efficiency, operation of electrochemical reactions and charge acceptance are influenced by the temperature [93]. Also higher temperature will be a cause for hazardous situations of lithium [27]. Therefore to maintain the temperature within the safe region, suitable cooling and heating systems are required. The operations of such cooling or heating systems depend on the battery-cell surface temperature and the internal temperature [69]. Battery SOC and ECM parameters are varied with the temperature and such variations should be taken into considerations for a better account of the battery behavior. In one approach, temperature can be considered as an input to the SOC estimation method. The ambient temperature alone is not sufficient enough to model the heat generation and heat transfer (conductive, convective and radiation) [27] to accurately represent thermal behavior.

As KF is suitable for linear system, EKF, UKF and CKF can be considered as an optimum state estimator for nonlinear systems such as li-ion battery systems. The advantage of KF based method is that it is not affected by the initial SOC error [97], but there are disadvantages such as high computational cost and complexity. Since these methods involve complex matrix operations, it is difficult to implement the algorithms in ordinary micro-controllers. Also they exhibits limitations such as linearization inaccuracy and uncertainties due to measurement noise. Even though the temperature is taken as an input for ECM based SOC estimation, KF methods do not consider the above mentioned heat generation and heat transfer. So applying KF methods with coupled electro-thermal battery model to calculate SOC and update OCV (of ECM) will require considerable time and computational cost.

The neural network method exhibits limitations such as errors due to the over-training, effects of the previous sample data set on the present data set and the existence of too many neurons. The risk of over-fitting increases due to the presence of excessive neurons while limited neurons will under-fit the data. Neural network method requires high computation as well as a large number of data set to train. Fuzzy logic method requires high computational cost, expertise knowledge as well as clearly defined fuzzy rules. The support vector machines method demonstrates the superiority over the

neural network method including no requirement to select the number of neurons, no requirement to identify the network topology and less problems regarding overfitting. Additionally, both neural network method and Support vector method present better results only for constant current situations and for dynamic situation the error is not in an acceptable level.

Hence non model based methods (direct measurement) are more suitable and among them OCV method and coulomb counting method are widely used. But adopting one of these methods alone may generate inaccuracy in results. Therefore combination of the OCV method and coulomb counting method is suggested as the SOC estimation method for the work in this thesis. The limitation of coulomb counting method can be overcome by adopting high accuracy current sensor and calculating the initial SOC value using the OCV-SOC method. The inputs are ambient temperature, current and OCV. The initial SOC is estimated using OCV-SOC method where the SOC values are stored using three dimensional table. The calculated SOC value will be an input to the electro-thermal model.

#### 2.3.4.2 Quantitative analysis

Error of the estimated value of SOC by indirect methods has been calculated against the coulomb counting method in previous research works. In calculating the value of SOC using the coulomb counting method, a high sensitivity calibrated current sensor has been used so that the integration error was minimal. LiFePO4 batteries have been tested under different temperature (0°C–60°C) and current profiles.

Neural network method emphasized that the Roots Mean Square (RMS) errors were within 4%, but the maximum error at some temperature ( 10°C–50°C) was larger than 10%. The errors are presented in the middle range of SOC (30%–80%). The most important fact is the inability of solving this problem by increasing the number of neurons or hidden layers because of the over-fitting of neural network [45]. As a different approach, the estimated SOC curve using neural network method has been compared with the reference SOC curve, estimated using coulomb counting method in terms of current disturbance response [71]. In the normal situation without a current disturbance, the RMS error was less than 0.006% which is acceptable, but for a dynamic situation with a current disturbance, even though the calculated SOC

converged to the reference value after some time, the deviation at the moment of the disturbance was at a considerable level.

In support vector method, for a normal condition the RMS error was over 5% where the maximum error was about 15%. For a dynamic situation error was about 2.5% where the maximum error was recorded as 13% [40]. For the fuzzy logic method the RMS error was roughly about 5% [60].

As for extended Kalman filter, the RMS error varied according to the adopted battery model [53]. For an example, for Thevenin model, the error was less than 0.6% which is acceptable. For the second order RC ECM the RMS value was close to 0.75% where the maximum error was close to 2% [72].

# 3 Thermal behavior of cylindrical batteries

To determine battery performance accurately and to estimate battery characteristics including lifetime, State of Charge (SOC) and State of Health (SOH), it is required to acquire an extensive battery model that reflects phenomena occurring within the battery [73]. In respect of battery phenomena, thermal behavior can be considered one of the most influential phenomenon to be reflected through comprehensive thermal modelling. In thermal modelling, it is essential to reflect how the ambient temperature, core temperature and surface temperature affect the battery performance, as well as the heat generation inside the battery [74] [75].

Because of various chemical, thermal and electrochemical reactions occur during the charging and discharging, heat is generated inside the battery. At deep discharging conditions, high current rates and other different environmental conditions, heat generation can substantially increase and so to maintain the temperature within the desire range, it is essential to obtain effective heat transfer mechanism, which includes heating and cooling. In the case of poor heat transfer, it can lead to thermal runaways [76].

Regarding battery temperature, high temperature (core temperature or surface temperature exceeding the safe upper temperature limits) and low temperature (core temperature or surface temperature lowering below the safe lower temperature limits) can cause adverse effects on the battery performance and characteristics including thermal runways, fire and explosion (see table 3.1) [76]. Safe temperature range slightly differs according to the cathode material of the lithium-ion battery and further

on the mode of operation, typically the discharging phase safe temperature range is about -20℃ to 60℃ and the charging phase it is about 0℃ to 40℃ [76].

### 3.1. Impact of temperature on lithium-ion batteries

Table 3.1: Impact of li-ion batteries [76]

| **Lower temperature effects** | **Higher temperature effects** |
|---|---|
| 1. Decrease of energy and power.<br>2. Chemical reactions will be slow down along with charge transfer velocity leading to reduction of ionic conductivity of electrolyte.<br>3. Reduction of battery capacity<br>4. Due to the deposit of lithium-ion on the electrode surface .<br>5. Increase in the internal resistance. | 1. Heat generation.<br>2. Thermal runway which leads to fire and explosion.<br>3. Decomposition of electrode materials.<br>4. Reduction of life time. (Including cycle aging and calendar aging.<br>5. Reduction in internal resistance.<br>6. Higher self-discharge. |

When batteries operate outside the desired temperature range, it causes hazardous consequences which affects the Battery Management System (BMS) functions [76]. Hence a precise representation of battery thermal behavior will ensure the performance, safety and lifespan of battery. There are many detailed thermal models, most of them are computationally exhaustive and inappropriate for the real time implementation. Most importantly, the thermal model must be able to anticipte the core temperature since it is crucial to determine the core temperature and its influence over other parameters of the model [75].

### 3.2. Battery Management System

The key function of a battery Management System (BMS) is maintaining the battery operation as smooth as possible by estimating the battery states including SOC, SOH, and such other characteristics as core temperature, surface temperature and coolant temperature; most importantly voltage and charging/discharging current while effectively communicating with the sub-systems of BMS [77]. The conventional or simplest BMS may only monitor the battery pack just to cater the power demand while preserving the temperature, charging/discharging current at the desired level, but an advanced BMS should consist of functions including fault diagnosis, lifetime degradation assessment and data acquisition and storage. The key functionalities of the BMS are identified below [75].

### 3.2.1. Management of battery charging/discharging current and voltage

The key function of a BMS is to avoid any abnormalities in the discharging/charging current as it may causes to fail not only the battery pack but also the other interconnected components. Having an accurate battery model along with an EMS will be beneficial to perform this task as it can monitor the deviation between measured data from the model along with the desired values [75].

### 3.2.2. Heat Management and operating temperature control

The main tasks of heat management and operating temperature control is continued operation of cooling and heating mechanisms to achieve an even distribution of the core and the surface temperatures of the battery pack. The temperature controlling block will give feedback to the cooling system/heating system when the battery pack temperature (core, surface) is not within the acceptable range. Cooling mechanism can be either active or passive where in passive cooling only the surrounding environment is employed and in active cooling some external cooling media is forced. As most of BMS have external cooling mechanisms that remove the heat at the surface, the righteous method is to remove the heat inside, because the maximum temperature is located inside the battery. Cooling media can be categorized as liquid cooling, air cooling and phase change (solid to liquid, liquid to gas). In the phase change cooling method, large amount of energy is released and absorbed when a phase change happened [78].

- Air cooling media : natural or forced air, cost beneficial, less complicated, low maintenance, light weight, low thermal conductivity
- Liquid cooling media: oil, direct cooling (the battery pack is submerged in the coolant), indirect cooling( the coolant flows around battery pack), leakages, structural complexity
- Phase change cooling (solid to liquid):
- Phase change cooling (liquid to gas):

## 4. The proposed comprehensive electro-thermal battery model

### 4.1. Overview of the proposed model

As stated before, an accurate battery model is very important to predict the behavior of a battery pack in a given application and thereby to identify the best battery management plan to preserve the long life of the battery.

Existing battery models are not comprehensive enough to accommodate the combined and inter-related electrical and thermal behavior of a battery, simultaneously. This limitation has led to significant modelling inaccuracies.

To address this vital gap, a new battery model is proposed in this research that has the following essential attribution.

1) Ability to model electrical and thermal responses simultaneously
2) Ability to model transient responses due to dynamics of battery charging and discharging currents
3) Ability to self-adapt battery parameters with changes in internal temperature.
4) Ability to model inherent hysteresis between charging and discharging currents.
5) Ability to present itself as a new block in MATLAB/Simulink for easy use by system designers and researchers.

The proposed battery model is based on second order ECM that has the ability to account for the dynamics of charging or discharging currents and the second order thermal model that has the ability to represent internal heat transfer and temperature.

Parameters of the ECM model are adapted by the model itself according to the State of internal temperature according to the electro-thermal data embedded within the model. Similar adoption of parameter is done to account for the parametric hysteresis charging and discharging state, that is as for the data embedded within the model. Figure 4.1.shows the appearance of MATLAB/Simulink block that presents the battery model. It has two power terminals and three outputs for information of SOC, core temperature ($T_C$) and surface temperature ($T_s$). Basic data for the battery is input through a mask as shown in figure 4.2. Other electro-thermal data that depends on the particular type of battery are fixed to the model and not recognized from the user.

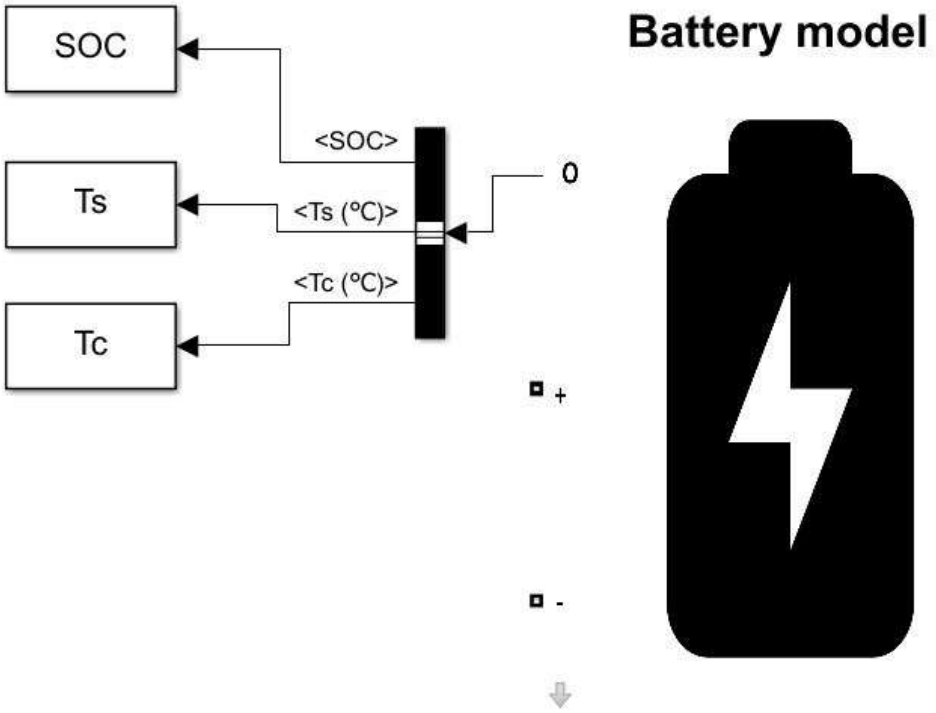


Figure 4.1: Overview of the proposed battery model

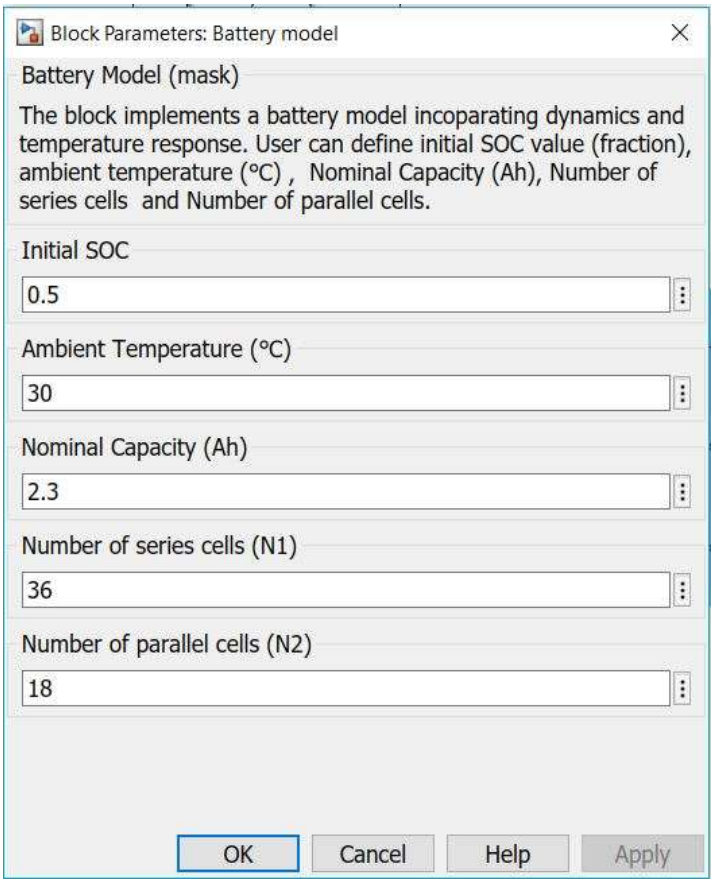


Figure 4.2: Battery model (mask)

The model consists of two parts; electrical model and thermal model which can be shown in figure 4.3 along with inputs, outputs and correlation of two models.

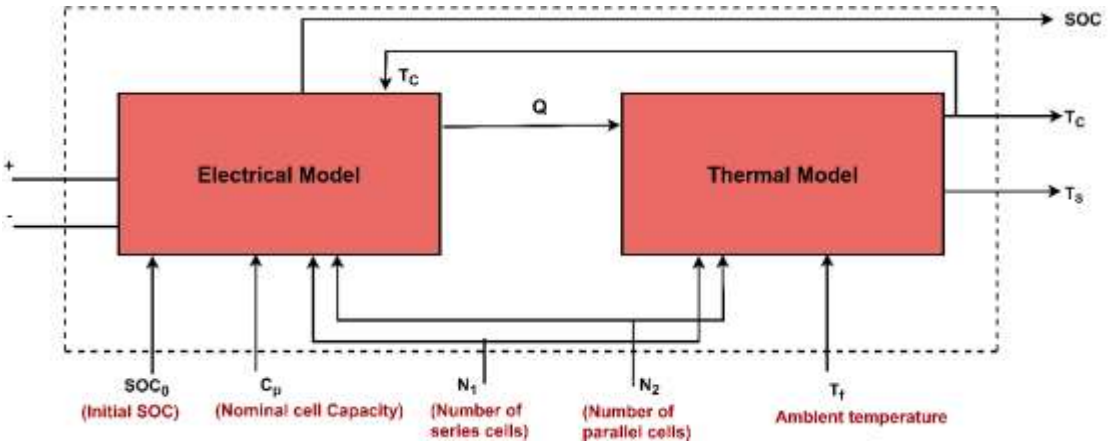


Figure 4.3: Coupling of electrical model and thermal model

Inputs $N_1$ (number of series cells) and $N_2$ (number of parallel cells) are common to both electrical and thermal models, $SOC_0$ (initial SOC0 and $C_p$ (nominal cell capacity) are inputs to electrical model and $T_f$ (ambient temperature) is an input

for the thermal model. The heat loss ($Q$) which is calculated from the electrical model is fed to the thermal model and $T_C$ of the thermal model is fed back to the electrical model. SOC is an output from the electrical model and $T_C$ and $T_s$ are outputs from the thermal model.

### 4.2. The electrical model (second order RC ECM)

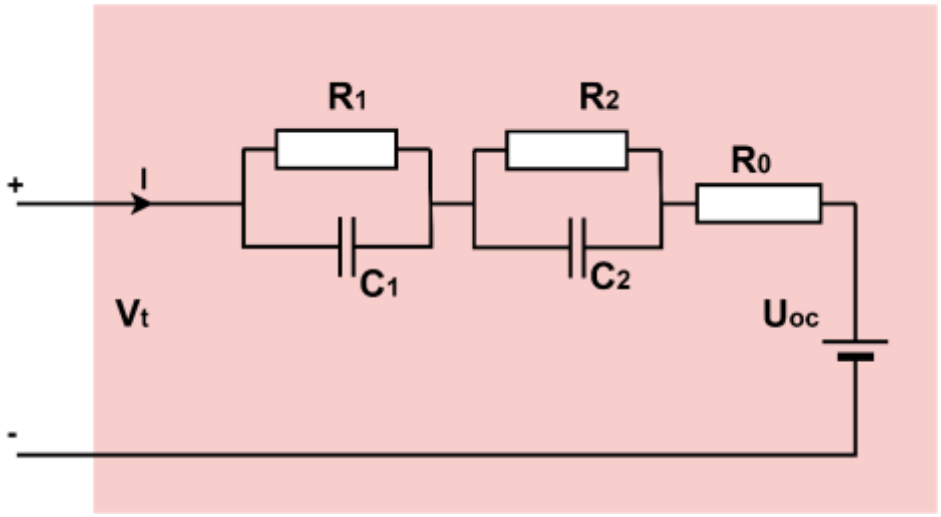


Figure 4.4: The second order RC ECM

Figure 4.4 shows the part of electrical model. This is second order RC Equivalent Circuit model (ECM), which consists of two number of RC branches, representing activation polarization and concentration polarization, with a series internal ohmic resistance. This ECM can model transient responses caused by dynamics of current/voltage applied on inputs. The more the number of RC branches the greater will be the closeness of the model to real behavior but the computational time will be greater. We stayed within the second order RC ECM as a compromise between the accuracy and computational time. First order ECM would have been computationally more efficient but it suffers from accuracy issues due to not accounting for the concentration polarization. Model parameters are functions of core temperature ($T_c$) and SOC, and listed below.

- $U_{oc}$ = Open Circuit Voltage (OCV)
- $R_o$ = Ohmic resistance (internal resistance)

- $R_1, C_1$ = Elements that model activation polarization. This branch models deviation in OCV due to the charge transfer dynamics inside the battery for conquering the impedance of the separator.
- $R_2, C_2$ = Elements that models concentration polarization. This branch models the voltage fall due to mass transfer dynamics within the cell.

Value wise, voltage drop across $R_1, C_1$ branch is greater than that across $R_2, C_2$ branch. Response wise $R_1, C_1$ branches is faster.

### 4.3. Thermal model (Two-State lumped Thermal model)

Figure 4.5 shows the thermal part of the battery model. This is two-state thermal model or second order lumped thermal model, which is an advanced model that predicts the core temperature and surface temperature. Here the heat generation is considered to a concentrated Joule heating at the core. To reduce the complexity, the effect of reversible entropic heat is omitted in the model since it is comparatively smaller compared to the total heat generation inside the battery. Also it assumes that the heat flux at the centre is negligible. Only the radial thermal dynamics are considered and the temperature variation along the axial direction is assumed homogeneous.

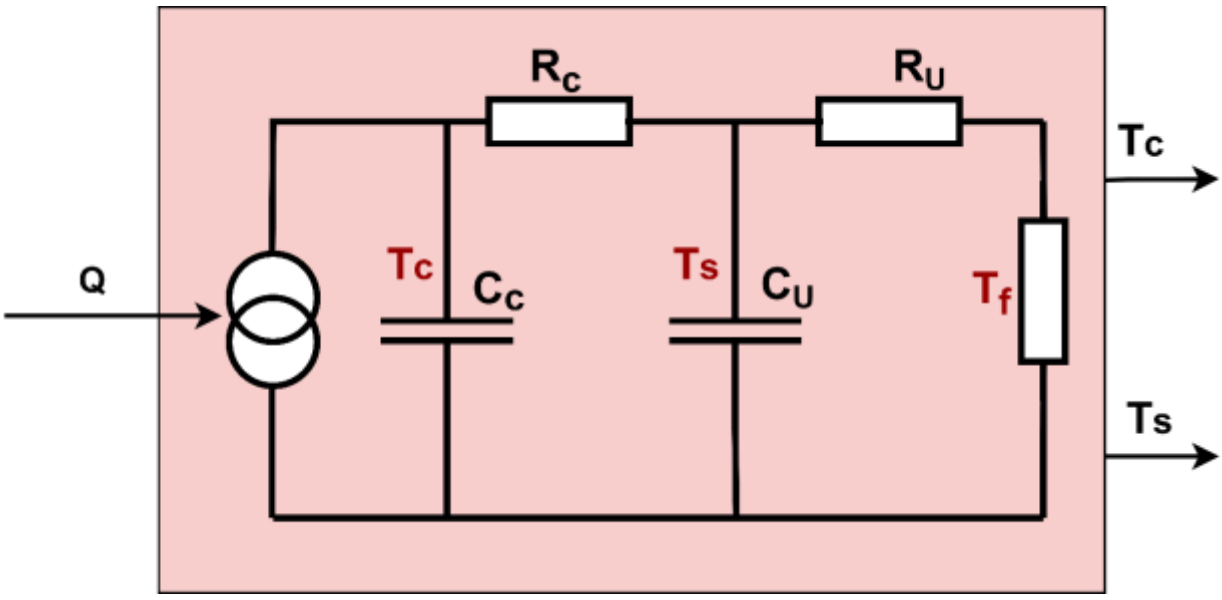


Figure 4.5: Two-state thermal model [74]

- $T_c$ = core temperature
- $T_s$ = Surface temperature

- $T_f$ = Ambient temperature
- $R_C$ = Thermal resistance that represents conduction heat transfer between core and surface
- $R_U$ = Thermal resistance that represents convection heat transfer between surface and ambient
- $C_C$ = Thermal capacitance that represents heat storage in the core.
- $C_U$ = Thermal capacitance that represents storage in the surface
- Q = Generated net heat

Capacitance $C_C$ and $C_S$ bring out thermal dynamics inside the battery. This complex mathematical model is given by the following equations (4.1), (4.2) and (4.3).

$$C_c \frac{dT_c}{dt} = Q + \frac{T_s - T_c}{R_c} \quad (4.1)$$

$$C_s \frac{dT_s}{dt} = \frac{T_f - T_s}{R_u} + \frac{T_c - T_s}{R_c} \quad (4.2)$$

$$Q = I * (V_t - V_{oc}) \quad (4.3)$$

Other parameters $R_C, R_U$ and $C_S$ are constant for a given battery cell. Values of parametric $R_U$ depends on the cooling system used for the battery according to the BMS. For the testing purposes, this was also assumed to be constant. Table 4.1 shows the values of different parameters for a single battery-cell. The corresponding values for the entire battery-pack is determined by knowing the number of cells in series ($N_1$) and the number such series-strings in parallel ($N_2$) in the battery pack. Figure 4.6 shows modelling basis.

Table 4.1: Thermal model parameters [74]

| Parameter | Value |
|---|---|
| $R_U\ (KW^{-1})$ | 3.19 |
| $R_C\ (KW^{-1})$ | 1.94 |
| $C_c\ (JK^{-1})$ | 62.7 |
| $C_s\ (JK^{-1})$ | 4.5 |

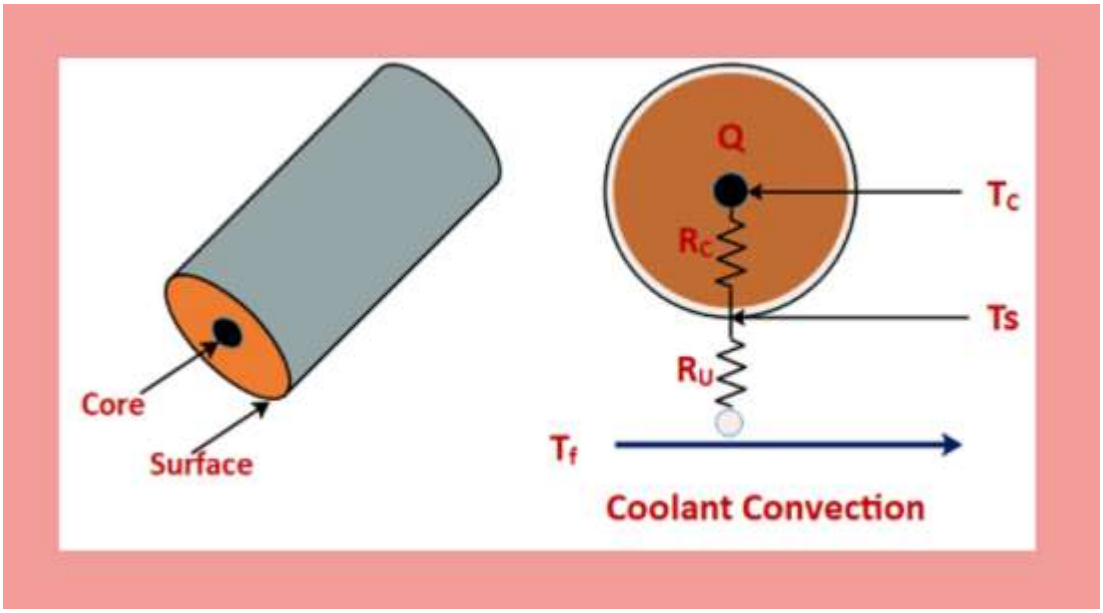


Figure 4.6: cylindrical single cell radial lumped thermal model [74]

### 4.4. Combining of electrical and thermal model

Figure 4.7 shows functional descriptions of the combined electrical and thermal models. The block that updates ECM parameter holds battery-type specific data for a single cell, namely 3D lookup tables for the values of $R_1$, $R_2$, $C_1$, $C_2$, $R_o$ and $V_{oc}$ for values of $T_C$ and SOC, for both state of charging (positive current) and discharging (negative current). Figure 4.8 shows the format of lookup for charging and discharging and figure 4.9 shows the stocking of different lookup tables in the block.

Similarly thermal parametric block holds basic thermal data for a single cell, for a particular battery type. Using inputs $N_1$ and $N_2$ the block computes $R_C$, $R_U$, $C_C$, $C_S$ for the entire battery pack (see table 4.3). Using the values of parameters, SOC and Q from the ECM model, and ambient temperature from the mask, the thermal model computes $T_C$ and $T_S$.

Table 4.2 : Thermal parameterization of battery pack

| | |
|---|---|
| $(R_U)_{pack} = {}^{1}/_{N_1 N_2} * (V_{oc})_{cell}$ | $(C_C)_{pack} = N_1 N_2 * (V_{oc})_{cell}$ |
| $(R_U)_{pack} = {}^{1}/_{N_1 N_2} * (V_{oc})_{cell}$ | $(C_S)_{pack} = N_1 N_2 * (V_{oc})_{cell}$ |

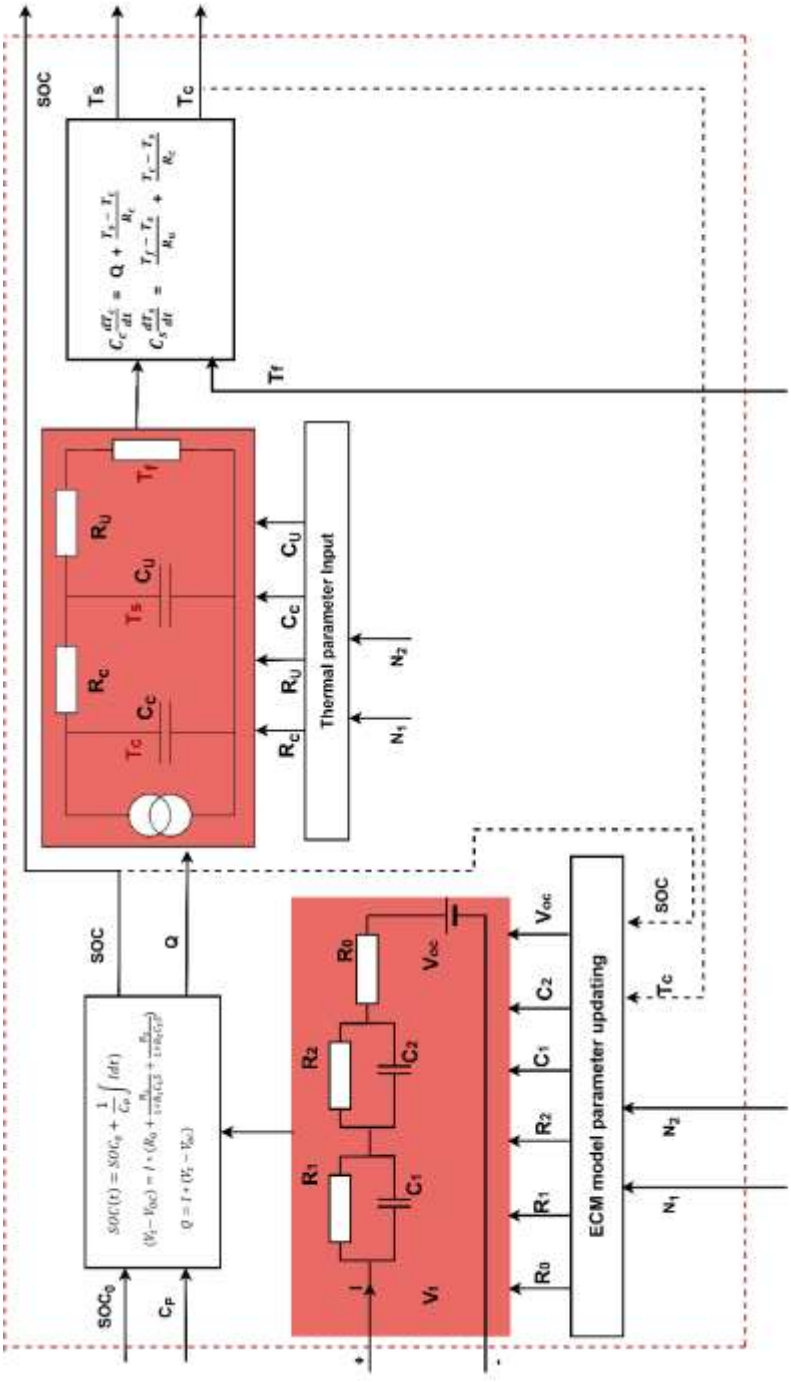


Figure 4.7: Combining of electrical model and thermal model

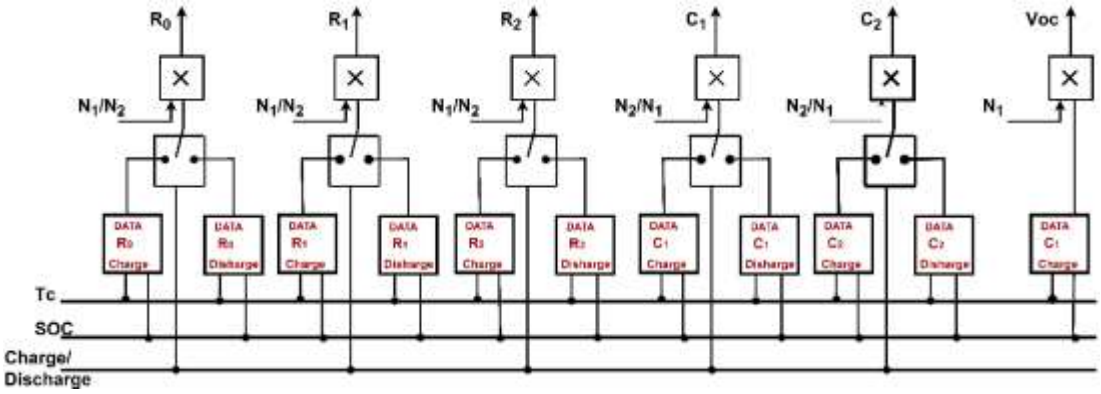


Figure 4.8 : Details of ECM parameter identification process

| SOC \ $T_C$ (°C) | 5 | 10 |
|---|---|---|
| 0.1 | $a_1$ | $b_1$ |
| 0.2 | $c_1$ | $d_1$ |

Charging

| SOC \ $T_C$ (°C) | 5 | 10 |
|---|---|---|
| 0.1 | $a_2$ | $b_2$ |
| 0.2 | $c_2$ | $d_2$ |

Discharging

Figure 4.9: ECM parameters at different SOC and $\boldsymbol{T_C}$ values

### 4.5. MATLAB/Simulink structure to represent battery as a circuit element

One of the important targets is to represent the battery model as a circuit element since it gives the user an effective and straightforward freedom to utilize the battery model in power systems and other applications to simulate, various scenarios, including implementation of BMS and EMS etc. Figure 4.10 shows the concept of modelling on a circuit element. The model provides three outputs of SOC, $T_C$ and $T_S$ from its output port, and other required outputs are directly measures at the input terminals, eg: $V_{in}$ , $I_{in}$ and $P_{in}$

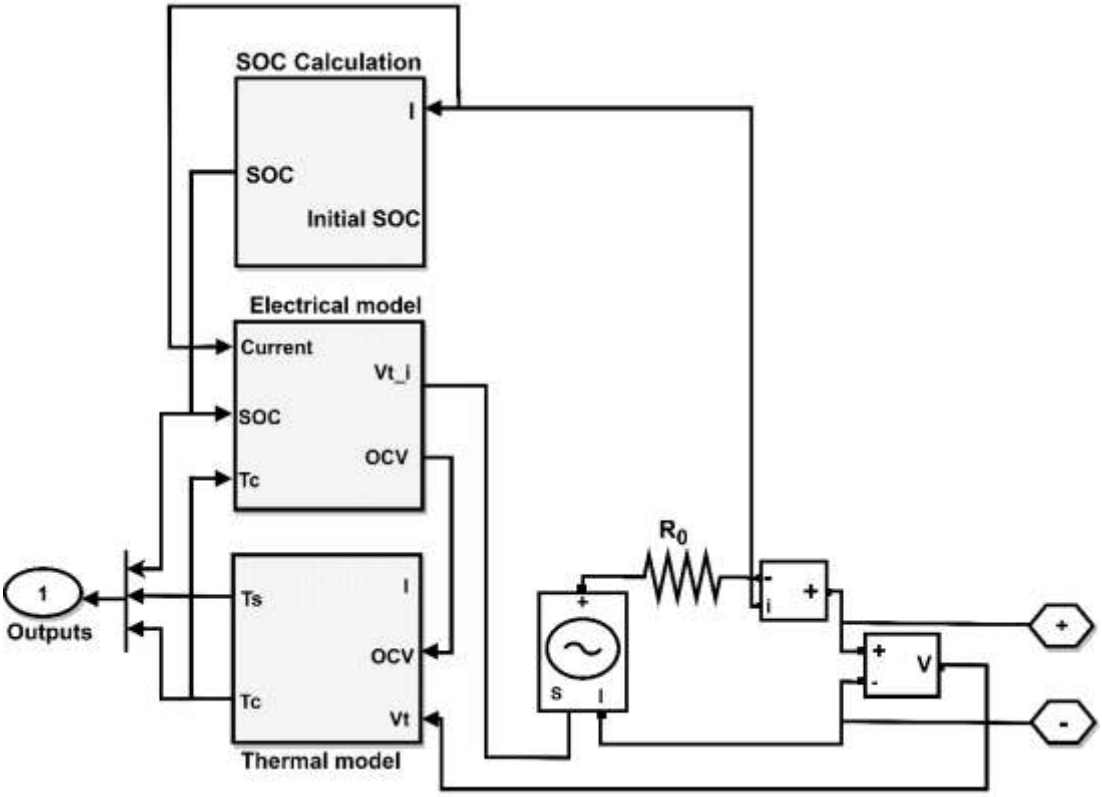


Figure 4.10: The proposed MATLAB model as a circuit element

The MATLAB/Simulink consists of three sub models which can be further divided in to sub sections performing the tasks listed in table 4.2.

Table 4.2: Sub-models of the proposed model

| | |
|---|---|
| Electrical model | SOC calculation model |
| | OCV calculation |
| | ECM model parameter calculation |
| | Terminal voltage calculation |
| | Heat loss calculation |
| Thermal model | Core and surface temperature calculation |

### 4.5.1. SOC calculation model

As the first stage, SOC is estimated using the coulomb counting method using inputs of applied current and initial SOC values as shown figure 4.11. $C_{rated}$ is a data supplied via mask, which represents Ampere-hour capacity of the battery cell.

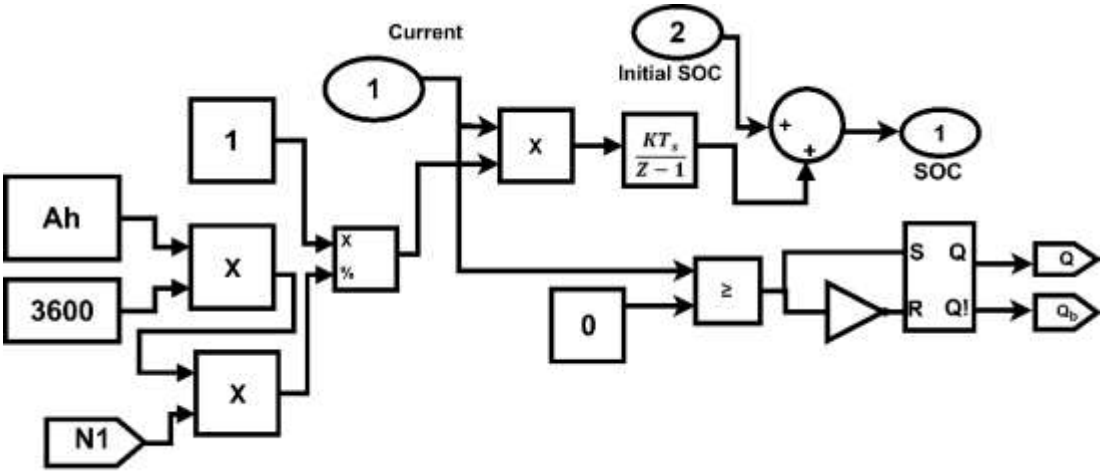


Figure 4.11: SOC calculation

Charging/ discharging state of the battery is identified using output Q and $Q_b$ where Q=1 for charging and $Q_b$=1 for discharging.

### 4.5.2 OCV calculation ($V_{oc}$)

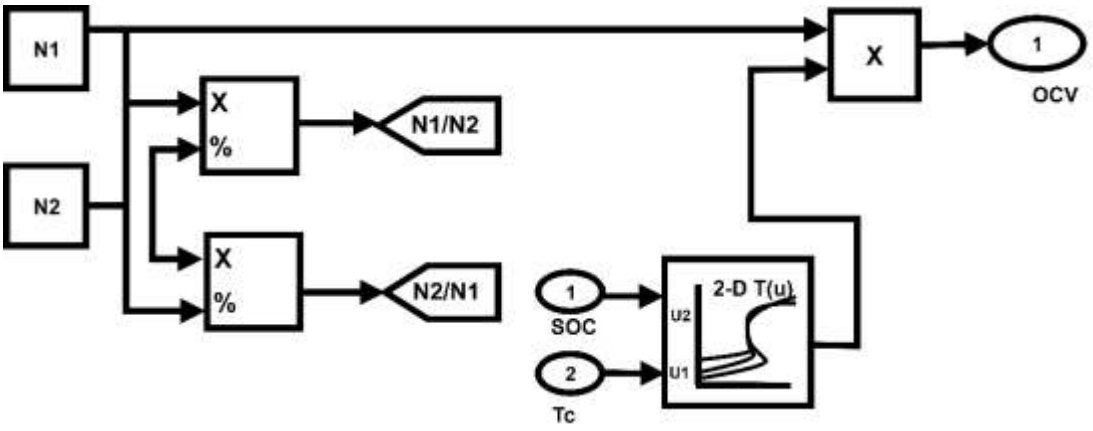


Figure 4.12: OCV calculation

The block estimates the value of OCV corresponding to the pair of $T_C$ and SOC using interpolations or extrapolations, on appropriate in terms of the nearest entity in the look up table. Here, we used linear interpolation (see figure 4.12). To obtain the OCV value for the battery pack, the cell-wise value is multiplied by $N_1$.

### 4.5.3. ECM parameter calculation

Each of $C_1$, $C_2$, $R_1$, $R_2$ and $R_s$ exhibits hysteresis between charging and discharging states. Therefore two lookup tables, one for charging state and the other for discharging state were stored for each parameter. Based on the polarity of the current (i.e. state of charging or discharging) the table is selected and then based on the SOC and $T_C$ the value is computed using interpolation (extrapolation, as appropriate) in terms of closest entries. Figure 4.13 shows the computations of capacitances, figure 4.14 computation of resistances ($R_s$) and figure 4.14 computation of $R_1$.

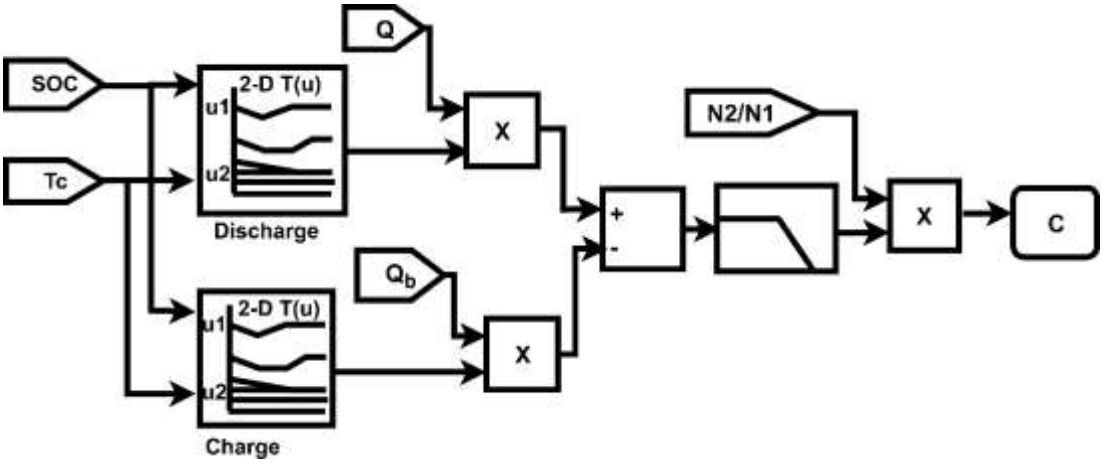


Figure 4.13: Capacitance ($C_1$ , $C_2$) calculation

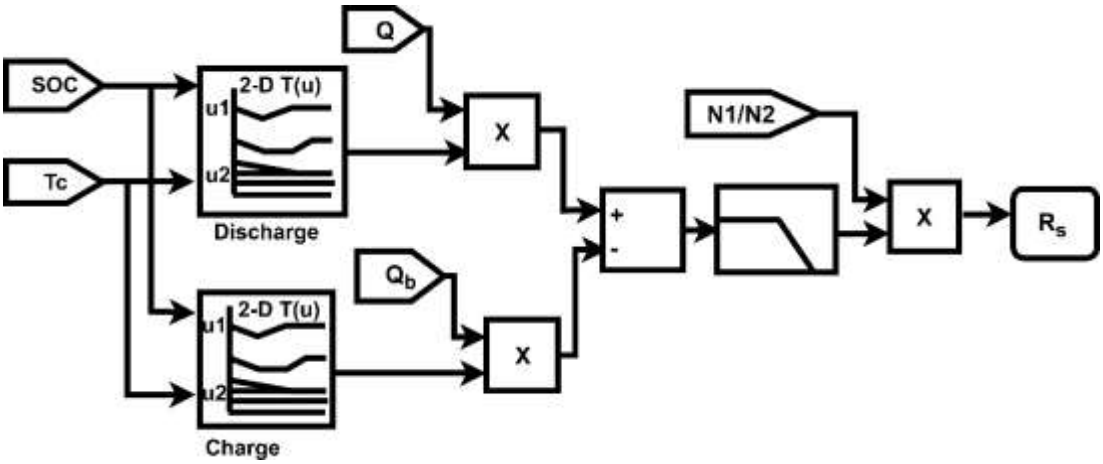


Figure 4.14: Resistance ($R_s$ ) calculation

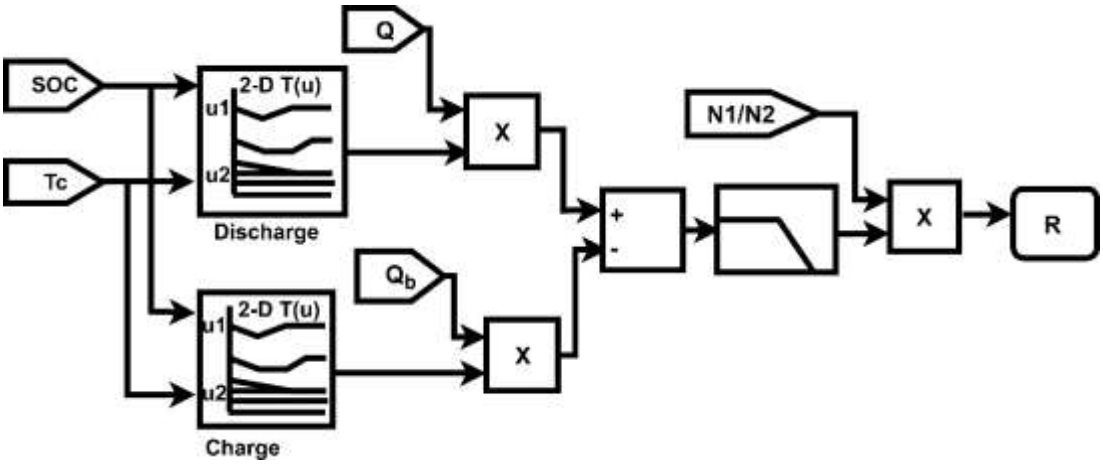


Figure 4.15: Resistance ($R_1$ , $R_2$ ) calculation

### 4.5.4 Terminal voltage calculation

Once ECM parameters are updated, terminal voltage $V_t$ for a given current is computed using the following mathematical expression (eq. 4.4), derived from the ECM model. Here Z-transform based computation is chosen to reduce the computational time. Figure 4.16 shows the terminal voltage calculation.

$$V_t(z) = V_{oc}(z) + \left(\frac{TR_1}{T+zR_1C_1}\right)I(z) + \left(\frac{TR_2}{T+zR_2C_2}\right)I(z) + R_sI(z) \qquad (4.4)$$

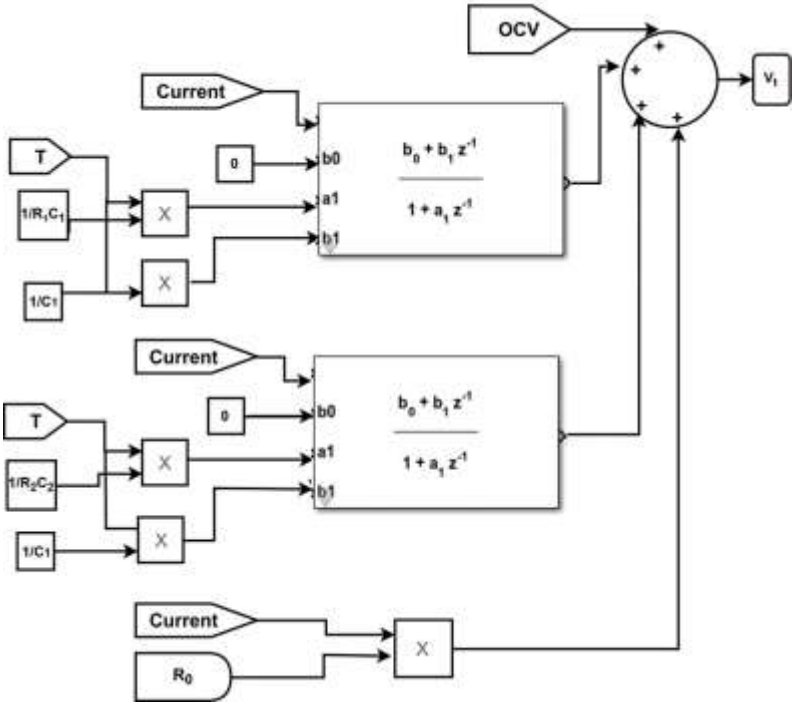


Figure 4.16: Terminal voltage ( $V_t$ ) calculation

### 4.5.5 Heat generation calculation (Q)

The heat generation is calculated taking the terminal voltage, current and OCV as inputs, shown in figure 4.17.

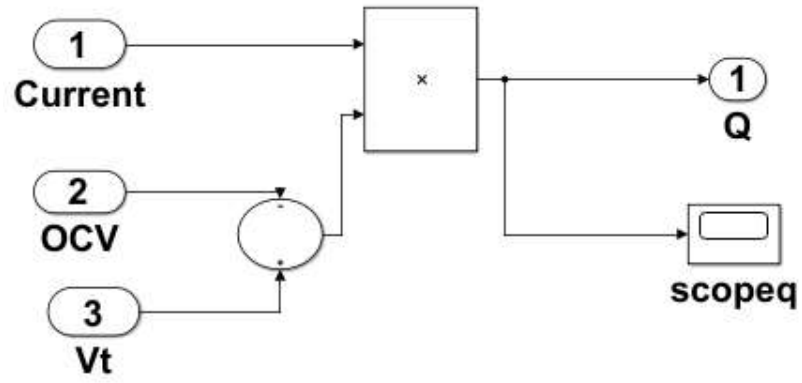


Figure 4.17: Heat calculation

### 4.5.6 Temperature calculation ($T_c$, $T_s$)

Core temperature ($T_c$) and surface temperature ($T_s$) are computed using the following mathematical expressions (equations 4.5 and 4.6), which were established from the thermal models. Heat generation (Q) and ambient temperature ($T_f$) are inputs. $T_{s(o)}$ and $T_{C(o)}$ are initial values of surface temperature and core temperature respectively which are two inputs. Figure 4.18 shows the computation of $T_c$ and $T_s$.

$$T_C(Z\left(\frac{(Z-1)R_C C_C+T}{TR_C C_C}\right) = \frac{Q(Z)}{C_C} + \frac{T_S(Z)}{R_C C_C} + \frac{ZT_C(0)}{T} \quad (4.5)$$

$$T_S(Z)(\frac{(Z-1)R_U C_S R_C+T(R_C+R_U)}{TR_U C_S R_C} = \frac{T_f(Z)}{R_U C_S}+\frac{T_C(Z)}{R_C C_S} + \frac{ZT_S(0)}{T} \quad (4.6)$$

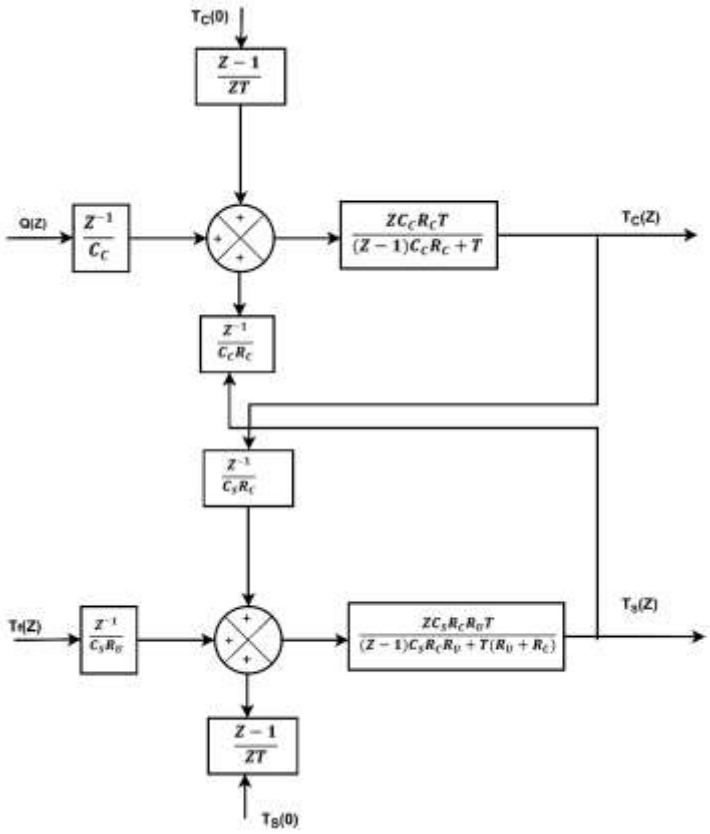


Figure 4.18: Temperature ( $T_c$ ,$T_s$ ) calculation

### 4.5.7 Considerations on the developed model

The developed model is comprehensive in accounting the dynamics of electrical and thermal performances of a battery including the parametric hysteresis between charging and discharging processes. In fact the basic model is representing one cell of the battery, and after providing inputs for the number of cell in series and parallel the model can update itself to represents the entire battery pack. So one of the underlying assumptions is that the cells are identical in all respects and there are no circulation current between parallel paths of cells inside the battery pack. In other words, the model assumes that appropriate other measures are in place in the battery pack to eliminate circulation current among parallel paths of cells.

If the requirement is to investigate the circulation current among the parallel paths, then cell-wise models should be used to represent individual cells in parallel paths accommodating tolerances in cell-parameters. This will be an attractive option of application of the developed model.

The developed model uses some data for the battery, obtained by prior tests conducted on the battery. These data are specific to the type and the capacity of the battery, so if a library of such data is maintained for different capacities and types the model can directly select the correct set at the simulations. This set of data includes the followings:

1) $R_S, R_1, R_2, C_1, C_2$ for different *SOC* and $T_C$ (under charging and discharging).
2) $V_{oc}$ for different *SOC* and $T_C$ (under charging and discharging ).
3) $R_U, R_C, C_c$ and $C_s$.

## 5. Testing of the developed battery model

In general, battery is part of the microgrid system undergoing charging and discharging events, as detailed by the overall energy management system of the microgrid. Often, the battery has to undergo fast and steep charging and discharging processes activated following sudden variation of output of distributed generation (i.e solar PV and wind) in the system and change in the load. Energy Management System should ensure that battery operation is restricted to the safe limits of the battery in particular the limits on SOC, limits on charging/discharging current (C-rate), limits on surface temperature or core temperature etc. To realize controlled charging and discharging, the battery must be fitted with a bidirectional power electronic converter having ability to transfer power in either direction.

### 5.1 Micro-grid layout

In order to test the performance of the developed battery model, battery system is considered as a part of a microgrid system along with renewable energy generations (solar PV and wind) and loads as shown in figure 5.1. It is assumed that the microgrid is connected to the grid. Typical daily profiles of the solar-PV, wind power and load are acquired which ensure both charging and discharging states for the battery in the full range. The operation with a selected energy management criteria over a span of one full day is considered. The system characteristics are in table 5.1.

Table 5.1: The system characteristics

| | | |
|---|---|---|
| Microgrid (kW) | 100 | |
| Battery | (maximum power) (kW) | 24 |
| | Nominal capacity (Ah) | 40 |
| | Maximum charging/discharging current (A) | 200 |

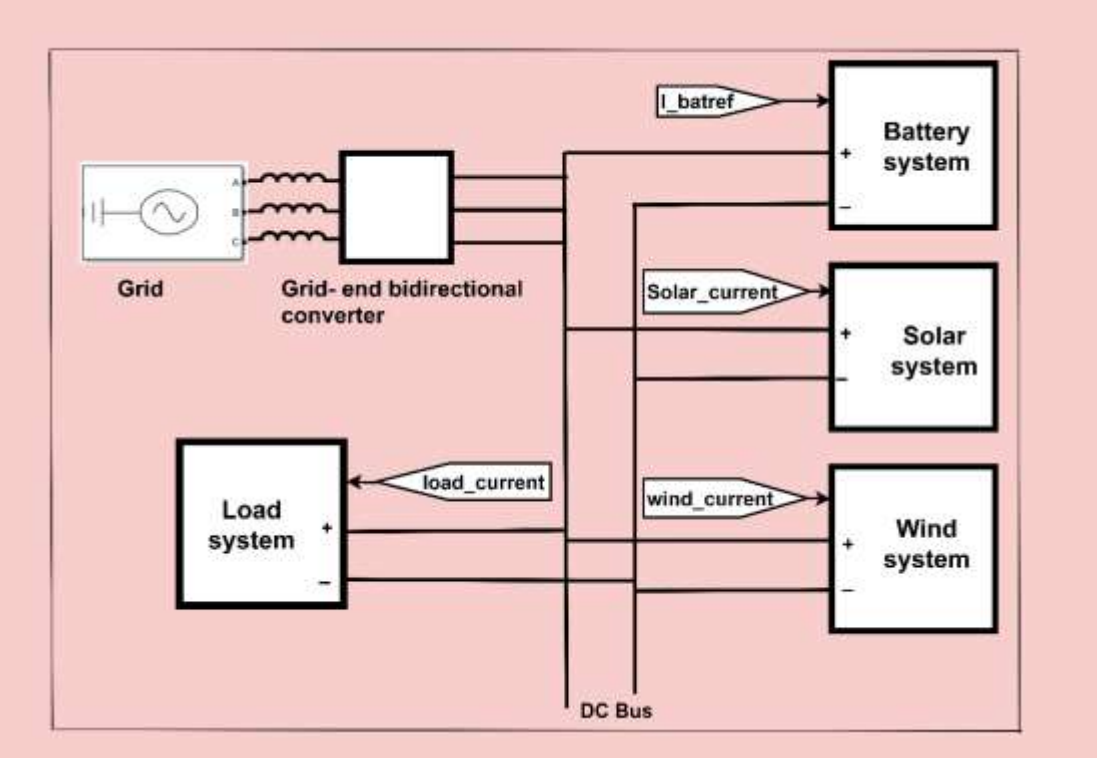


Figure 5.1: The configuration of the proposed battery test system

As shown in figure 5.1, battery system, load system, solar system and wind system are connected to the DC bus and the grid is connected through a separate grid –end bidirectional AC/DC converter.

### 5.2. Energy Management Criteria

Energy management criteria determines the extent of charging and discharging current subjected to the specified limits on SOC, $T_S$ ($T_C$) and power. For this implementation, $T_S$ was chosen to specify thermal limits due to the ease of measuring the surface temperature. $T_S$ = 60°C was the thermal limit, beyond which battery current is forced to zero. SOC range was restricted to 0.3 and 0.9 in that the battery will be charged only if the battery SOC is less than 0.9 and battery will be discharged only if SOC is greater than 0.3. Since the battery maximum power is limited to 24kW, the maximum charging/discharging current is limited to 200A. When the wind and solar generation exceeds the load the battery is charged according to the respective rate and when the renewable generation cannot meet the load, the battery is discharged according to the required rate. Furthermore the excess/deficit power that the battery cannot handle is sent/taken to or from the grid. The test microgrid is a DC grid with a DC backbone of 220V.

### 5.2.1 Energy Management Algorithm

Figure 5.2 illustrates the chosen energy management criteria in terms of a flowchart.

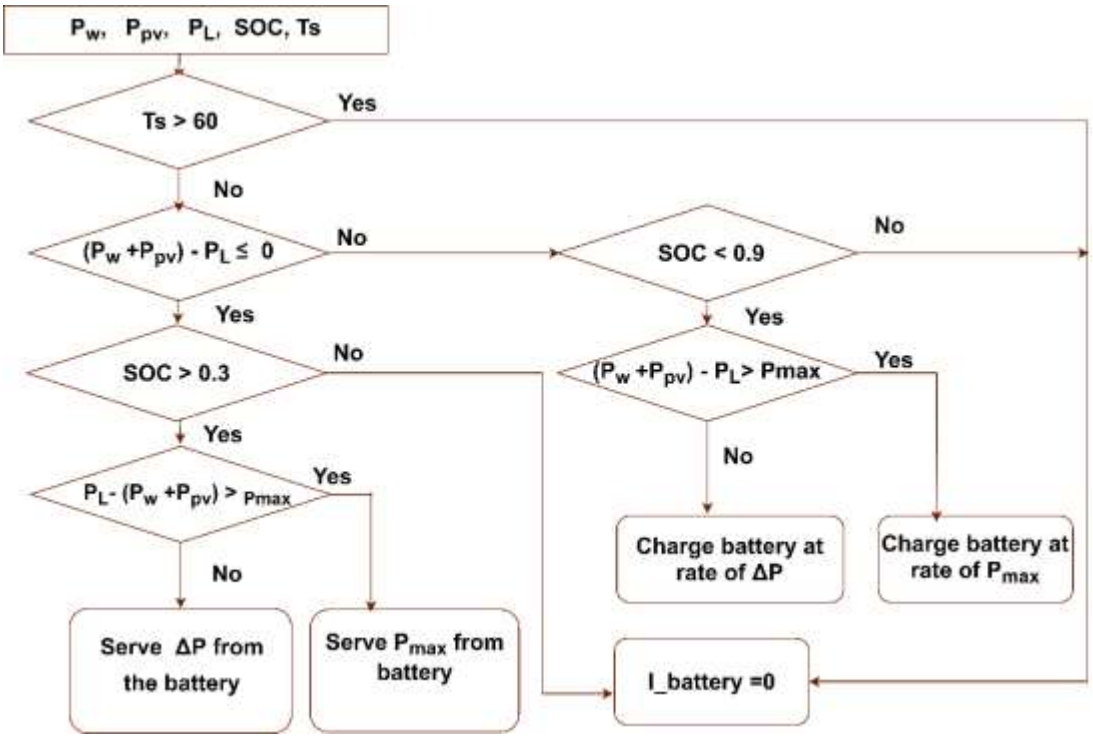


Figure 5.2: Energy Management Algorithm

The algorithm, receives solar power, wind power, load, SOC and $T_s$ as inputs. As given in the flowchart, there are four distinct cases for charging and discharging of the battery, when $T_s$ < 60℃.

1) Case 1: Excess generation and SOC< 0.9

$$\Delta P = (P_{PV} + P_W) - P_L \quad (5.1)$$

$$I_{charge} = \begin{cases} \frac{\Delta P}{220}, & \Delta P \leq 24 \text{ kW} \\ \frac{24000}{220}, & \Delta P > 24 \text{ kW} \end{cases} \quad (5.2)$$

2) Case 2: Excess generation and SOC > 0.9

$$I_{charge} = 0 \quad (5.3)$$

3) Case 3: Less generation and SOC > 0.3

$$\Delta P = P_L - (P_{PV} + P_W) \quad (5.4)$$

$$I_{discharge} = \begin{cases} -\frac{\Delta P}{220}, & \Delta P \leq 24 \text{ kW} \\ -\frac{24000}{220}, & \Delta P > 24 \text{ kW} \end{cases} \quad (5.5)$$

4) Case 4: Less generation and SOC < 0.3

$$I_{discharge} = 0 \quad (5.6)$$

MATLAB code that implements the algorithm is given in Appendix B.

### 5.2.2. Battery System

As stated below, the battery is supplied with a bidirectional converter, which in this case is a bidirectional DC-DC converter. At one end is 220V DC bus and at the other end 120V battery. The converter uses a mid- DC link architecture with a 350V DC bus supplied with an energy storage capacitor. The 220V bus end converter is controlled to give an input current equal to that commanded by the energy management algorithm. Depending on whether there is a charging current or discharging current, the mid DC link capacitor voltage rises up or falls down respectively. The battery end converter is sensitive to the DC-link voltage and it always acts to regulate the DC-link voltage at the pre-set value of 350V by either giving energy from the capacitor or transferring energy to the battery. Then two converter, as a whole, implement the required energy transfer between the 220V bus and the battery at the respective voltage levels.

Control wise, 220V bus end converter is operating on current control PWM, and the battery end converter is closed loop voltage control with internal current loop control using hysteresis current control.

The PI compensator at the battery end converter plays an important role in maintaining the DC-link voltage at 350V with response time compatible with the rate of change of power in the distributed generation.

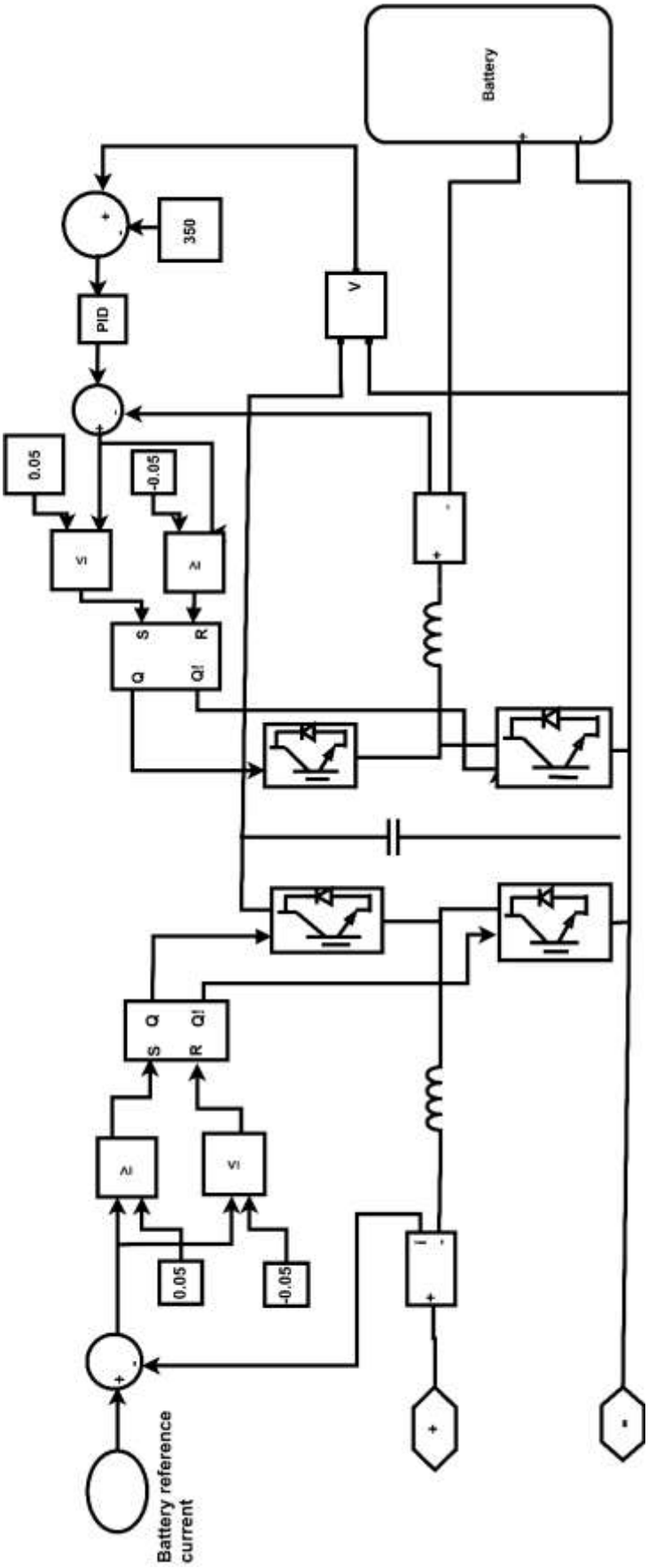


Figure 5.3: Battery system

### 5.2.3. Grid-end bidirectional converter

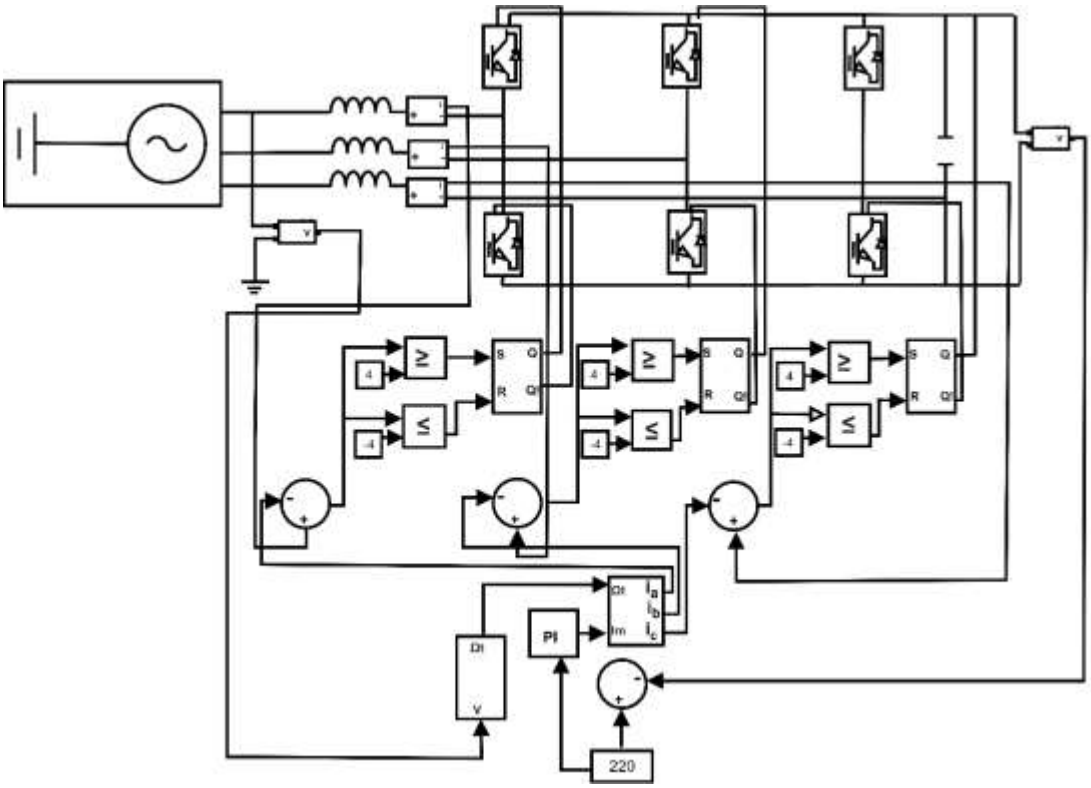


Figure 5.5: Grid-end bidirectional converter

- Three-phase bidirectional AC/AC converter
- Controller regulates voltage across output capacitor at 220V by drawing/returning sinusoidal current from the grid
- Controller determines magnitude of current according to deviation of output voltage from 220V through PI controller
- Hysteresis current controller is used to implement current

Grid end converter is a bidirectional AC/DC converter. Its primary task is to maintain the DC bus voltage at 220V, irrespective of changes in generation, load, and battery operation at all times. This converter has to take power from the AC grid when there is a net deficit of power in the microgrid, or return power back to the AC grid when there is a net excess of power in the microgrid. This can happen when there is an excess generation of a time when battery SOC is already at its upper limit at 0.9, or deficit of generation at a time when the battery SOC at its lower limit of 0.3. In all times, the current at the AC grid side is maintained in phase with the voltage (unity p.f.) while

the current waveforms are synthesized to be sinusoidal. This operation is ensured by the control implemented on the converter.

### 5.2.4. Modelling of renewable generations and loads

Renewable sources were modelled on controlled current sources injecting power into the 220V DC bus. To represent typical daily profile of generation, extracted power data from real sources were stored lookup tables to determine the instantaneous current reference for the controlled current source over a span of day.

Loads were also modelled in the same way but current now not injected to the bus, it is absorbing from the bus.

Figure 5.6, 5.7 and 5.8 show the model of wind, PV source and load.

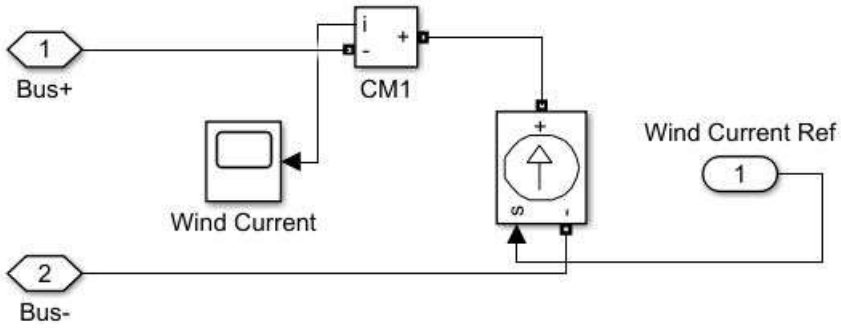


Figure 5.6: Wind model

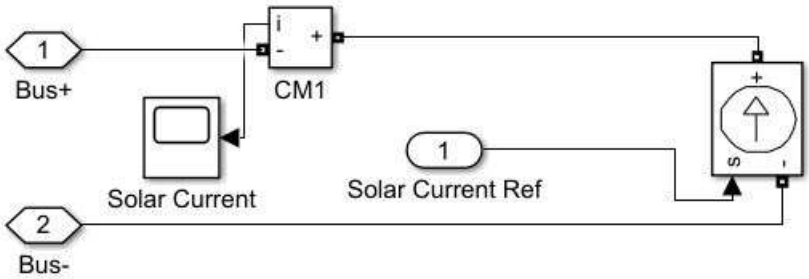


Figure 5.7: Solar model

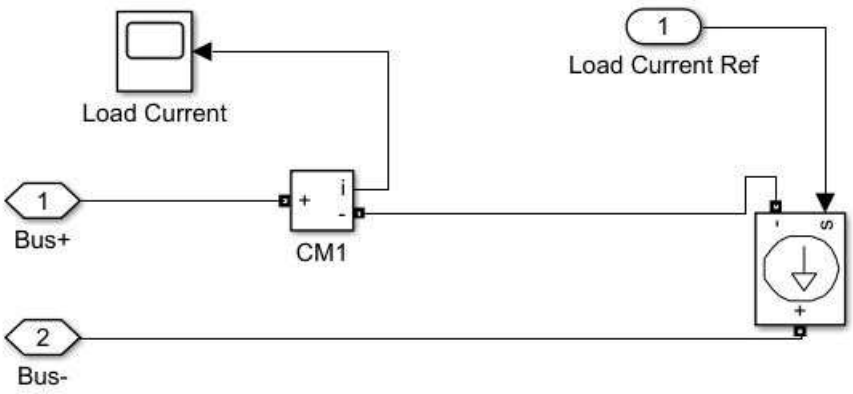


Figure 5.8: Load model

The power variation of the renewable energies (wind and solar) and load are shown in the following table 5.2.

Table 5.2: Renewable energy and load power variation

| | |
|---|---|
| Solar (kW) | $0 < P_{pv} < 31.6$ |
| Wind (kW) | $30 < P_w < 60$ |
| Load (kW) | $22 < P_L < 85$ |

Current references for the source and loads were determined by the respective power values in the look up tables at that point of time.

The equations (5.9), (5.10) and (5.11) shows how current references were computed from power references.

$$I_{ref\_wind} = \frac{P_{wind}}{220} \qquad \textbf{(5.9)}$$

$$I_{ref\_solar} = \frac{P_{solar}}{220} \qquad \textbf{(5.10)}$$

$$I_{ref\_load} = \frac{P_{load}}{220} \qquad \textbf{(5.11)}$$

# 6 Simulation results

## 6.1 Battery data

As stated before, some data specific to the type and capacity of the battery are required to be stored within the model. These data are obtained by prior tests conducted on such types and capacities of batteries. For the simulations described below, a set of data found in the literature [75] is used (see Appendix A). This set included data on the parameters $R_S, R_1, R_2, C_1, C_2$ and their variations with *SOC* and $T_C$, variation of $V_{oc}$ with *SOC* and $T_C$ (under both charging and discharging states), and thermal parameters $R_U$, $R_C$, $C_c$ and $C_s$.

### 6.1.1 Variation of resistance ($R_S, R_1, R_2$) values with SOC and $T_C$

The variation of resistances ($R_S, R_1, R_2$) with SOC and $T_C$ was obtained using 2-D cubic line interpolation to obtain the continuously differentiable surface plot seen in the figure 6.1, figure 6.2 and figure 6.3 respectively. It can be seen that there is an increase in the resistance values as the SOC increases. At lower SOC and higher SOC, the variation of values of resistances is significant and at the middle SOC range, the variation of values of resistances is less. Also the resistance values significantly depend on the temperature.

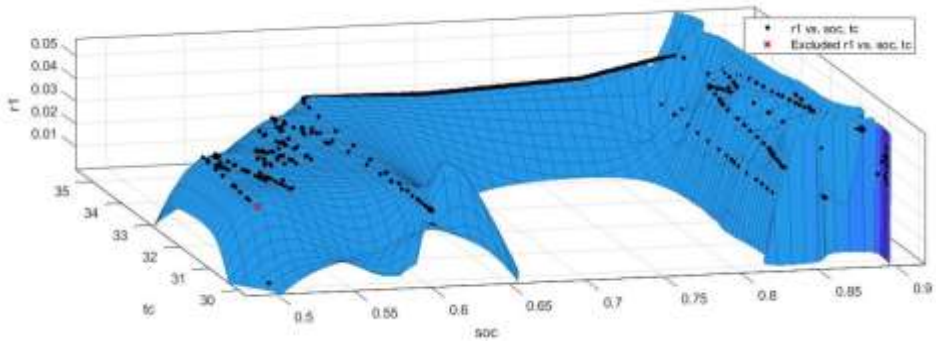


Figure 6.1: variation of $R_1$ with SOC and $T_C$

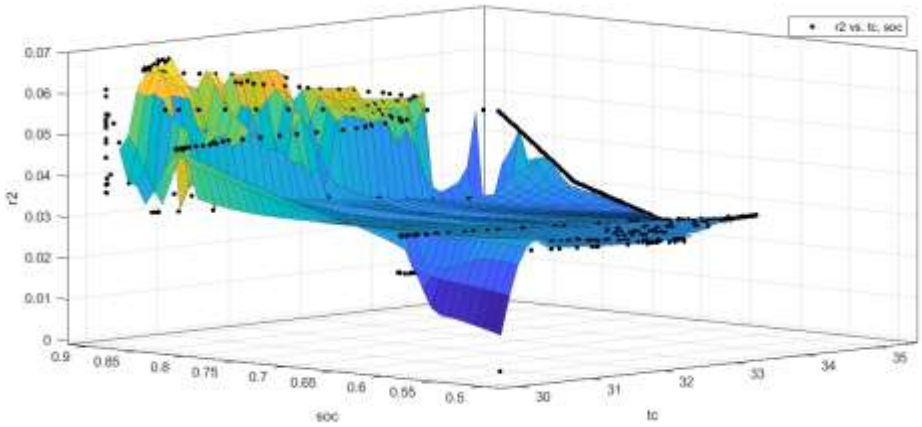


Figure 6.2: variation of $\mathbf{R_2}$ with SOC and $\boldsymbol{T_C}$

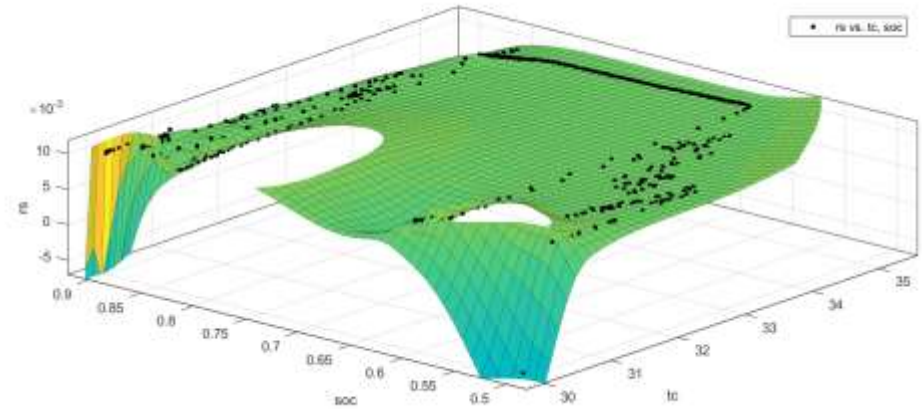


Figure 6.3: variation of $\mathbf{R_s}$ with SOC and $\boldsymbol{T_C}$

### 6.1.2 Variation of capacitances ( $C_1, C_2$) values with SOC and $T_C$

The variation of capacitances ( $C_1, C_2$) with SOC and $T_C$ was obtained using 2-D cubic line interpolation to obtain the continuously differentiable surface plot seen in the figure 6.4 and figure 6.5 respectively. It can be seen that there is an increase in the capacitance values as the SOC increases. At lower SOC and higher SOC, the variation of values of capacitances is significant and at the middle SOC range, the variation of values of capacitances is less. Also values significant depends on temperature.

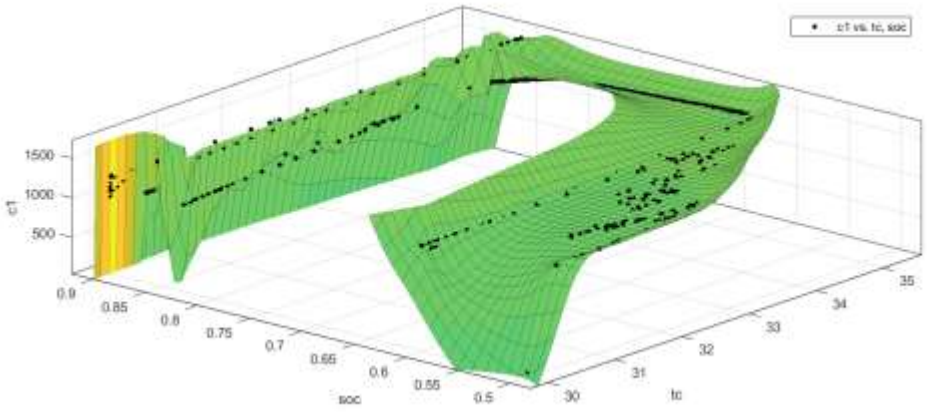


Figure 6.4: variation of $\mathbf{C_1}$ with SOC and $\boldsymbol{T_C}$

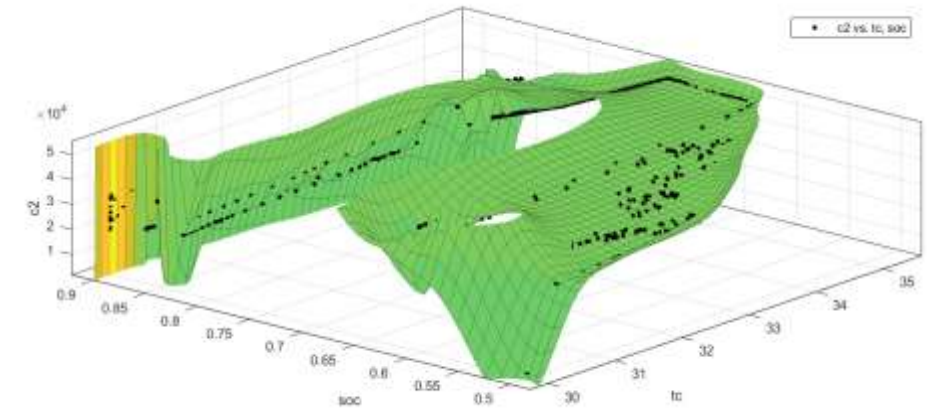


Figure 6.5: variation of $\mathbf{C_2}$ with SOC and $\boldsymbol{T_C}$

### 6.1.3 Variation of open circuit voltage ($V_{oc}$) values with SOC and $T_C$

The variation of OCV with SOC and $T_C$ was obtained using 2-D cubic line interpolation to obtain the continuously differentiable surface plot seen in the figure 6.6. It can be seen that there is an increase in OCV value as the SOC increases. At lower SOC and higher SOC, the variation of OCV is significant and at the middle SOC range, the variation of OCV is less. Also OCV value significant depends on temperature.

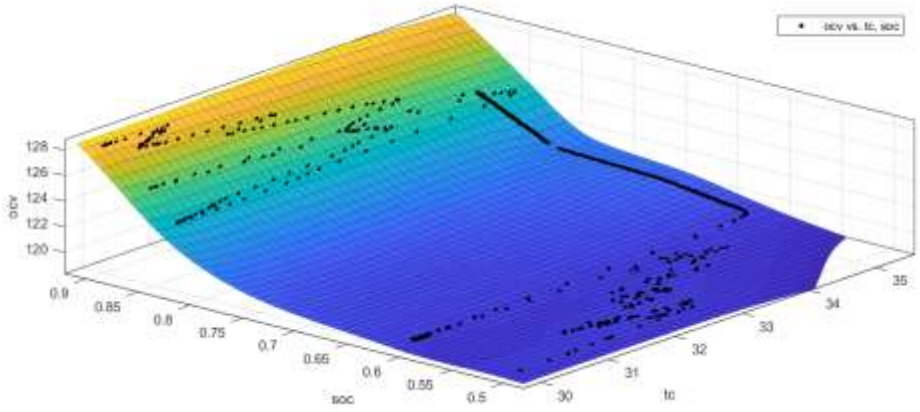


Figure 6.6: variation of **OCV** with SOC and $T_C$

## 6.2 Battery response (Electro-thermal dynamics)

The proposed electro-thermal battery model was tested in the micro-grid setup in MATLAB/Simulink with variable renewable energy and load profiles covering the span of one full day, as shown in figure 6.7. The daily load profile (which has two peaks naming morning peak and evening peak), wind power profile and solar profile were scaled to ensure typical charging/ discharging events over the day.

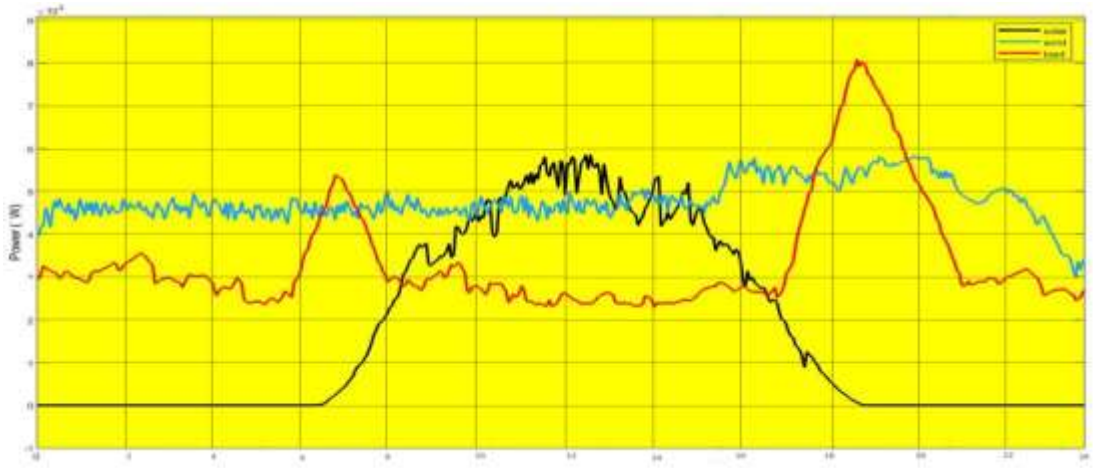

Figure 6.7: Renewable Energy Profiles

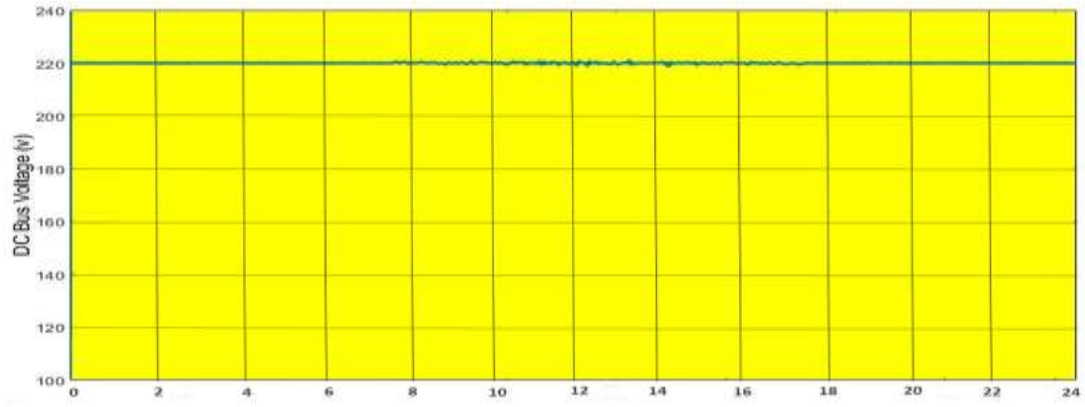


Figure 6.8: DC bus voltage

According to the figure 6.8, it can be observed that the DC bus voltage is maintained at 220V irrespective of the variations of generation, load and battery operation. This indicates that the micro-grid is operating healthily as a platform for the tests of BMS.

Figure 6.9 shows the traces of battery current, battery SOC, battery terminal voltage, battery core-temperature and battery surface-temperature over the day.

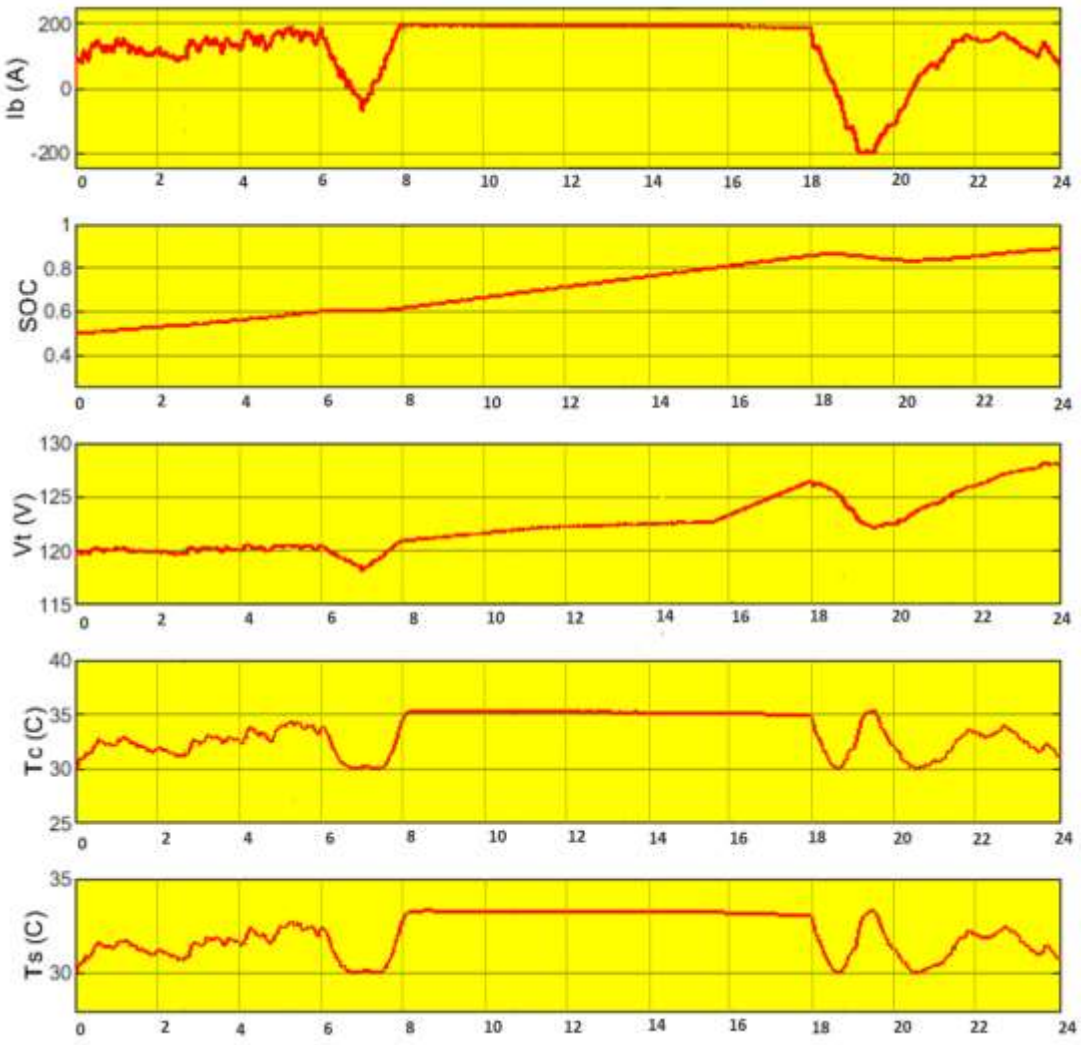


Figure 6.9: Simulation results

### $I_b$ (Battery current)

With reference to battery current profile, it could be noticed that the battery discharged at two time periods (hour 6-8 and 18-22) where battery current became negative value. During the hour 18-22, the battery discharged with the maximum discharging current (200A) as the generations could not meet the load. During the hour, 8-18, battery charges at the maximum rate as the generations exceeded the load.

### State Of Charge (SOC)

The initial SOC value was assumed as 0.5. During the two intervals, where battery discharged (hour 6-8 and 18-22), the SOC value of the battery decreased and the other times SOC value increased.

**Terminal voltage ($V_t$)**

The terminal voltage varies between about 117V and 128V. Over the two discharging intervals (hour 6-8 and 18-22), terminal voltage decreases. With times, terminal voltage varies in accordance with the battery current and variation of ECM parameters.

**Core temperature ($T_C$)**

Core temperature varies approximately between 30℃ and 35℃. The initial core temperature is taken as the ambient temperature (30℃). During times when the battery is charging at constant current, the core temperature is also remains steady at 35℃.

**Surface temperature ($T_S$)**

Surface temperature varies approximately between 30℃ and 32℃. The initial surface temperature was taken as the ambient temperature (30℃). The variation of surface temperature has a close follow up of the variation of the core temperature as expected.

Figure 6.10 shows the variations in the battery parameters $R_0$, $R_1$, $R_2$, $C_1$ and $C_2$ during the day.

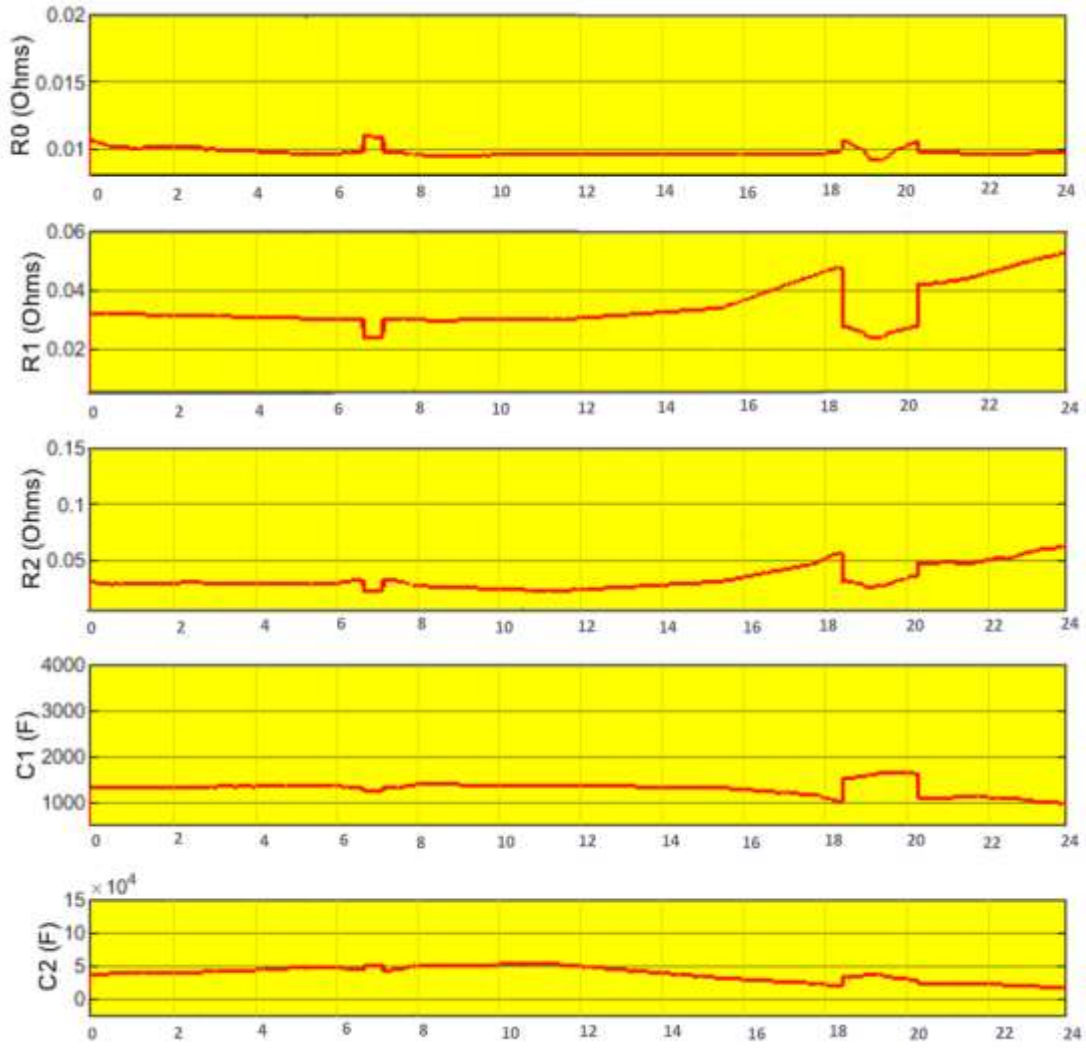


Figure 6.10: Simulation results (ii)

**Resistance ($R_o, R_1, R_2$) values variation with time**

It can be clearly seen that resistances are varying with time, according to the level of SOC, core temperature and state of operation, i.e. charging or discharging. It is apparent that charging/discharging hysteresis is having a significant impact.

**Resistance ($C_1, C_2$) values variation with time**

Capacitances are also varying with time, on evident in the graph. These changes are also governed by the level of SOC, core temperature and state of charging/discharging.

# 7 Conclusion and future work

## 7.1 Conclusion

The need of a computationally efficient battery model capable of accounting for the dynamics of electrical and thermal performances simultaneously has been long felt, especially, in the designing of battery energy storage systems for micro-grids involving renewable energy sources, and in electric vehicles. Thermal impacts and its influence on battery performance are two crucial aspects that must be accounted for ensuring the safety and longevity of batteries. Beside this vital fact, not a single battery-model available so far had accounted for the combined electrical and thermal responses. Moreover, the inherent hysteresis exhibited by battery performance between charging and discharging states must also be incorporated within the model if the model is to be more accurate. One of the reasons for this bottleneck is the high computational time.

This thesis presented details of the development of a computationally efficient combined and comprehensive electro-thermal battery model, incorporating the hysteresis between charging and discharging states. The conclusions that can be drawn out of this work are:

1) A comprehensive battery model incorporating electro-thermal combined behavior and charging-discharging hysteresis has been developed.
2) The developed model is computationally efficient.
3) The developed model is user friendly, because it is presented as a circuit component in MATLAB Simulink.
4) The model is easily adaptable to individual battery banks using relevant battery pack-data.

The battery model is a two-terminal block in Simulink that can be connected to the external system. Therefore, the dynamics of terminal voltage and input current are directly measurable. Three separate outputs of the block give the instantaneous values of SOC, core-temperature and surface-temperature. Input data to the model are provided through a mask, which are initial SOC, numbers of cells in series and parallel in the pack, ambient temperature, and nominal cell capacity.

Development of a micro-grid platform to test the performance of batteries under real world conditions was another parallel task presented in this thesis. The micro-grid was having a common DC-busbar to which the grid is connected via a bidirectional AC-DC converter, battery bank is connected via a bidirectional DC-DC converter and solar PV inverters, wind power inverters and loads were connected directly. AC-DC converter was tasked to regulate the voltage of the DC busbar against changes in the generation and consumption in the micro-grid by either taking or returning power from or to the grid. A separate energy management criterion determined the instantaneous charging and discharging current for the battery bank within its stipulated safe limits, which the DC-DC converter was tasked to establish. Simulation of the battery bank with the developed battery model within the micro-grid over the course of a typical day, involving charging and discharging revealed that the predicted performance of the battery was a close match of the true behavior of the the battery. Also, the simulation times were acceptably lower, indicating that the model was computationally efficient.

### 7.2 Future work

An important further work will be a development of a test bench containing a thermal chamber, programmable DC current supply, programmable DC load, precision current and voltage sensors, fast data acquisition system and a host computer, as in figure 7.1. This test bench can then be used to obtain data for the model of a given type and capacity of a battery.

Parameter $R_S$ of the thermal model will change if batteries are cooled with an external cooling system. Therefore, the effective value of $R_S$ under different cooling conditions needs to be estimated and adopted accordingly.

Ambient temperature can vary over the time depending on climatic and other causes. Therefore, the value of ambient temperature input in the model should be updated appropriately to match with what actually encountered in practice.

To make the battery model a still better model, battery degradation factors should also be included into the battery model. This requires operation-specific battery aging experiments involving advanced test facilities, which may take several months or years.

Finally, for a realistic validation of the battery model, the practical measurements of $T_S, T_C, V_t$ and SOC for an applied profile of input current over a period of time should be compared with the simulated results on the same input current over the same period of time. For this purpose, the chosen battery-bank should be pre-tested for the model data and then simulate. This again comes to the need of a test bench of Fig. 7.1.

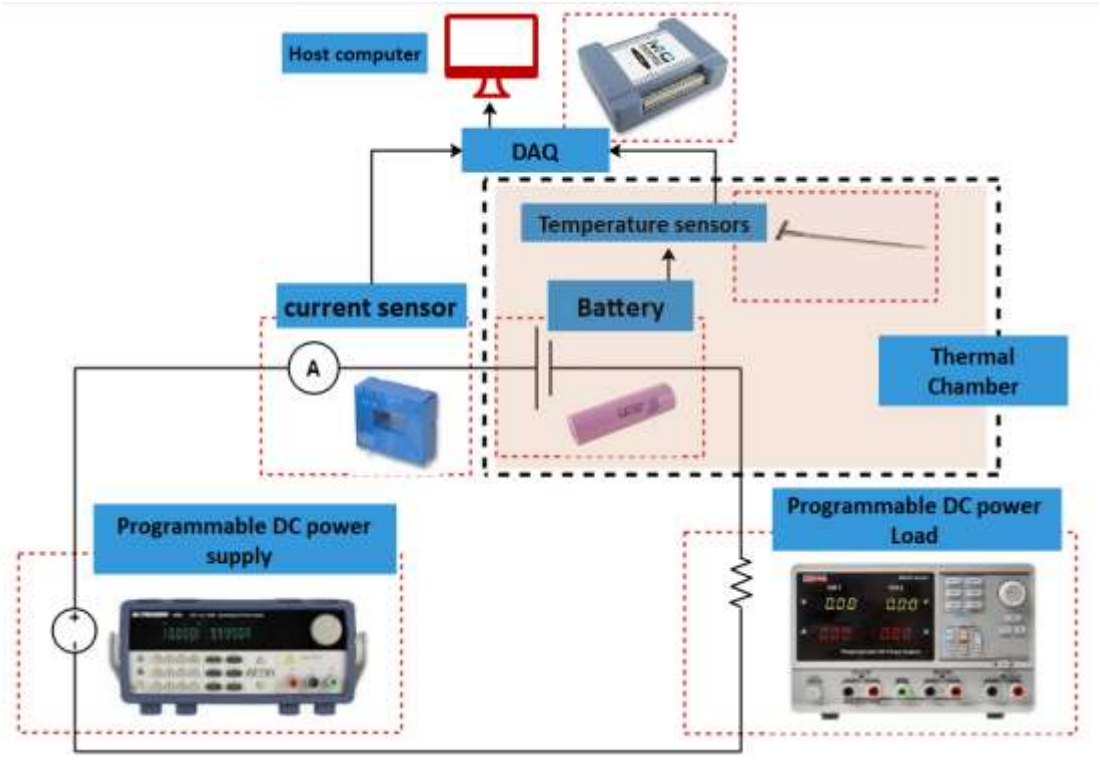


Figure 7.1: Battery test bench

## REFERENCES

[1] Lawder, M. T., Suthar, B., Northrop, P. W., De, S., Hoff, C. M., Leitermann, O., ... & Subramanian, V. R. (2014). Battery energy storage system (BESS) and

battery management system (BMS) for grid-scale applications. *Proceedings of the IEEE*, *102*(6), 1014-1030.

[2] Awasthi, A., Karthikeyan, V., Das, V., Rajasekar, S., & Singh, A. K. (2017). Energy Storage Systems in Solar-Wind Hybrid Renewable Systems. In Smart Energy Grid Design for Island Countries (pp. 189-222). Springer, Cham.

[3] Farrokhabadi, M., König, S., Cañizares, C. A., Bhattacharya, K., & Leibfried, T. (2017). Battery energy storage system models for microgrid stability analysis and dynamic simulation. IEEE Transactions on Power Systems, 33(2), 2301-2312.

[4] Faisal, M., Hannan, M. A., Ker, P. J., Hussain, A., Mansor, M. B., & Blaabjerg, F. (2018). Review of energy storage system technologies in microgrid applications: Issues and challenges. Ieee Access, 6, 35143-35164.

[5] Alharbi, H. (2015). Optimal Planning and Scheduling of Battery Energy Storage Systems for Isolated Microgrids (Master's thesis, University of Waterloo).

[6] Divya, K. C., & Østergaard, J. (2009). Battery energy storage technology for power systems—An overview. Electric power systems research, 79(4), 511-520.

[7] Sarasua, A. E., Molina, M. G., & Mercado, P. E. (2013). Dynamic modelling of advanced battery energy storage system for grid-tied ac microgrid applications. Energy Storage-Technologies and Applications.

[8] Naeinian, B. (2016). Seamless Operation of a Microgrid Using BESS.

[9] Rivera-Barrera, J. P., Muñoz-Galeano, N., & Sarmiento-Maldonado, H. O. (2017). SoC estimation for lithium-ion batteries: Review and future challenges. Electronics, 6(4), 102.

[10] Zubi, G., Dufo-López, R., Carvalho, M., & Pasaoglu, G. (2018). The lithium-ion battery: State of the art and future perspectives. Renewable and Sustainable Energy Reviews, 89, 292-308.

[11] Zhang, R., Xia, B., Li, B., Cao, L., Lai, Y., Zheng, W., ... & Wang, W. (2018). State of the art of lithium-ion battery soc estimation for electrical vehicles. Energies, 11(7), 1820.

[12] Meng, J., Luo, G., Ricco, M., Swierczynski, M., Stroe, D. I., & Teodorescu, R. (2018). Overview of lithium-ion battery modeling methods for state-of-charge estimation in electrical vehicles. Applied Sciences, 8(5), 659.

[13] Mathew, M., Mastali, M., Catton, J., Samadani, E., Janhunen, S., & Fowler, M. (2018). Development of an electro-thermal model for electric vehicles using a design of experiments approach. Batteries, 4(2), 29.

[14] Borase, P. B., & Akolkar, S. M. (2017, August). Energy management system for microgrid with power quality improvement. In 2017 International conference on Microelectronic Devices, Circuits and Systems (ICMDCS) (pp. 1-6). IEEE.

[15] Gunasekaran, M., Mohamed Ismail, H., Chokkalingam, B., Mihet-Popa, L., & Padmanaban, S. (2018). Energy management strategy for rural communities' DC micro grid power system structure with maximum penetration of renewable energy sources. Applied Sciences, 8(4), 585.

[16] Hernández, A. C. L. (2017). Energy Management Systems for Microgrids Equipped with Renewable Energy Sources and Battery Units (Doctoral dissertation, Aalborg Universitetsforlag).

[17] Tsang, K. M., Chan, W. L., Wong, Y. K., & Sun, L. (2010, August). Lithium-ion battery models for computer simulation. In 2010 IEEE International Conference on Automation and Logistics (pp. 98-102). IEEE.

[18] Hu, X., Li, S., & Peng, H. (2012). A comparative study of equivalent circuit models for Li-ion batteries. Journal of Power Sources, 198, 359-367.

[19] Dey, S., Ayalew, B., & Pisu, P. (2014, December). Adaptive observer design for a Li-ion cell based on coupled electrochemical-thermal model. In ASME 2014 Dynamic Systems and Control Conference. American Society of Mechanical Engineers Digital Collection.

[20] Moura, S. J., Krstic, M., & Chaturvedi, N. A. (2013, September). Adaptive PDE observer for battery SOC/SOH estimation. In ASME 2012 5th Annual Dynamic Systems and Control Conference joint with the JSME 2012 11th Motion and Vibration Conference (pp. 101-110). American Society of Mechanical Engineers Digital Collection.

[21] He, H., Xiong, R., & Fan, J. (2011). Evaluation of lithium-ion battery equivalent circuit models for state of charge estimation by an experimental approach. energies, 4(4), 582-598.

[22] Wu, B., & Chen, B. (2014, September). Study the performance of battery models for hybrid electric vehicles. In 2014 IEEE/ASME 10th International Conference on Mechatronic and Embedded Systems and Applications (MESA) (pp. 1-6). IEEE.

[23] Raël, S., Urbain, M., & Renaudineau, H. (2014, June). A mathematical lithium-ion battery model implemented in an electrical engineering simulation software.

In 2014 IEEE 23rd International Symposium on Industrial Electronics (ISIE) (pp. 1760-1765). IEEE.

[24] Feng, J., He, Y. L., & Wang, G. F. (2013). Comparison study of equivalent circuit model of Li-Ion battery for electrical vehicles. Res. J. Appl. Sci. Eng. Technol, 6, 3756-3759.

[25] Fang, J., Qiu, L., & Li, X. (2017). Comparative study of Thevenin model and GNL simplified model based on kalman filter in SOC estimation. International Journal of Advanced Research in Computer Engineering & Technology (IJARCET) Volume, 6.

[26] Chen, B., Ma, H., Fang, H., Fan, H., Luo, K., & Fan, B. (2014, August). An approach for state of charge estimation of Li-ion battery based on Thevenin equivalent circuit model. In 2014 Prognostics and System Health Management Conference (PHM-2014 Hunan) (pp. 647-652). IEEE.

[27] Xiong, R., Cao, J., Yu, Q., He, H., & Sun, F. (2017). Critical review on the battery state of charge estimation methods for electric vehicles. Ieee Access, 6, 1832-1843.

[28] Ren, H., Zhao, Y., Chen, S., & Wang, T. (2019). Design and implementation of a battery management system with active charge balance based on the SOC and SOH online estimation. Energy, 166, 908-917.

[29] Coleman, M., Lee, C. K., Zhu, C., & Hurley, W. G. (2007). State-of-charge determination from EMF voltage estimation: Using impedance, terminal voltage, and current for lead-acid and lithium-ion batteries. IEEE Transactions on industrial electronics, 54(5), 2550-2557.

[30] Dey, S., Ayalew, B., & Pisu, P. (2015). Nonlinear robust observers for state-of-charge estimation of lithium-ion cells based on a reduced electrochemical model. IEEE Transactions on Control Systems Technology, 23(5), 1935-1942.

[31] Xie, B., Liu, Y., Ji, Y., & Wang, J. (2018). Two-stage battery energy storage system (bess) in ac microgrids with balanced state-of-charge and guaranteed small-signal stability. Energies, 11(2), 322.

[32] He, H., Xiong, R., Zhang, X., Sun, F., & Fan, J. (2011). State-of-charge estimation of the lithium-ion battery using an adaptive extended Kalman filter based on an improved Thevenin model. IEEE Transactions on vehicular technology, 60(4), 1461-1469.

[33] Chang, W. Y. (2013). The state of charge estimating methods for battery: A review. ISRN Applied Mathematics, 2013.

[34] Barai, A., Widanage, W. D., Marco, J., McGordon, A., & Jennings, P. (2015). A study of the open circuit voltage characterization technique and hysteresis assessment of lithium-ion cells. Journal of Power Sources, 295, 99-107.

[35] Lee, S., Kim, J., Lee, J., & Cho, B. H. (2008). State-of-charge and capacity estimation of lithium-ion battery using a new open-circuit voltage versus state-of-charge. Journal of power sources, 185(2), 1367-1373.

[36] Cheng, Z., Wang, L., Liu, J., & Lv, J. (2016). Estimation of state of charge of lithium-ion battery based on photovoltaic generation energy storage system. Tehnički vjesnik, 23(3), 695-700.

[37] Weng, C., Sun, J., & Peng, H. (2014, March). An open-circuit-voltage model of lithium-ion batteries for effective incremental capacity analysis. In ASME 2013 dynamic systems and control conference. American Society of Mechanical Engineers Digital Collection.

[38] Ma, Y., Zhou, X., Li, B., & Chen, H. (2016). Fractional modeling and SOC estimation of lithium-ion battery. IEEE/CAA Journal of Automatica Sinica, 3(3), 281-287.

[39] Ng, K. S., Moo, C. S., Chen, Y. P., & Hsieh, Y. C. (2009). Enhanced coulomb counting method for estimating state-of-charge and state-of-health of lithium-ion batteries. Applied energy, 86(9), 1506-1511.

[40] Hansen, T., & Wang, C. J. (2005). Support vector based battery state of charge estimator. Journal of Power Sources, 141(2), 351-358

[41] Tudoroiu, R. E., Zaheeruddin, M., Radu, S. M., & Tudoroiu, N. (2018). Real-Time Implementation of an Extended Kalman Filter and a PI Observer for State Estimation of Rechargeable Li-Ion Batteries in Hybrid Electric Vehicle Applications—A Case Study. Batteries, 4(2), 19.

[42] Linghu, J., Kang, L., Liu, M., Jin, W., & Rao, H. (2018, November). State of charge estimation for ternary battery in electric vehicles using spherical simplex-radial cubature kalman filter. In 2018 International Conference on Power System Technology (POWERCON) (pp. 1586-1592). IEEE.

[43] Wu, T. H., & Moo, C. S. (2017). State-of-charge estimation with state-of-health calibration for lithium-ion batteries. Energies, 10(7), 987.

[44] Li, Y., Zou, C., Berecibar, M., Nanini-Maury, E., Chan, J. C. W., van den Bossche, P., ... & Omar, N. (2018). Random forest regression for online capacity estimation of lithium-ion batteries. Applied energy, 232, 197-210.

[45] He, W., Williard, N., Chen, C., & Pecht, M. (2014). State of charge estimation for Li-ion batteries using neural network modeling and unscented Kalman filter-based error cancellation. International Journal of Electrical Power & Energy Systems, 62, 783-791.

[46] Yan, Q., & Wang, Y. (2017, July). Predicting for power battery SOC based on neural network. In 2017 36th Chinese Control Conference (CCC) (pp. 4140-4143). IEEE.

[47] Yu, D. X., & Gao, Y. X. (2013). SOC estimation of Lithium-ion battery based on Kalman filter algorithm. In Applied Mechanics and Materials (Vol. 347, pp. 1852-1855). Trans Tech Publications.

[48] Tingting, D., Jun, L., Fuquan, Z., Yi, Y., & Qiqian, J. (2011, May). Analysis on the influence of measurement error on state of charge estimation of LiFePO4 power Battery. In 2011 International Conference on Materials for Renewable Energy & Environment (Vol. 1, pp. 644-649). IEEE.

[49] He, Z., Gao, M., Wang, C., Wang, L., & Liu, Y. (2013). Adaptive state of charge estimation for Li-ion batteries based on an unscented Kalman filter with an enhanced battery model. Energies, 6(8), 4134-4151.

[50] Hussein, A. A. (2014). Kalman filters versus neural networks in battery state-of-charge estimation: A comparative study. International Journal of Modern Nonlinear Theory and Application, 3(05), 199.

[51] Dişçi, F. N., El-Kahlout, Y., & Balıkçı, A. (2017, November). Li-ion battery modeling and SOC estimation using extended Kalman filter. In 2017 10th International Conference on Electrical and Electronics Engineering (ELECO) (pp. 166-169). IEEE.

[52] Huria, T., Ceraolo, M., Gazzarri, J., & Jackey, R. (2013). Simplified extended kalman filter observer for soc estimation of commercial power-oriented lfp lithium battery cells (No. 2013-01-1544). SAE Technical Paper.

[53] Plett, G. L. (2003). Advances in EKF SOC estimation for LiPB HEV battery packs. Consultant to Compact Power, Inc.

[54] Lu, J., Chen, Z., Yang, Y., & Lv, M. (2018). Online estimation of state of power for lithium-ion batteries in electric vehicles using genetic algorithm. IEEE Access, 6, 20868-20880.

[55] He, W., Williard, N., Chen, C., & Pecht, M. (2013). State of charge estimation for electric vehicle batteries using unscented kalman filtering. Microelectronics Reliability, 53(6), 840-847.

[56] Ma, Y., Duan, P., Sun, Y., & Chen, H. (2018). Equalization of lithium-ion battery pack based on fuzzy logic control in electric vehicle. IEEE Transactions on Industrial Electronics, 65(8), 6762-6771.

[57] Gan, L., Yang, F., Shi, Y. F., & He, H. L. (2017, November). Lithium-ion battery state of function estimation based on fuzzy logic algorithm with associated variables. In IOP Conference Series: Earth and Environmental Science (Vol. 94, No. 1, p. 012133).

[58] Singh, P., & Reisner, D. (2002, October). Fuzzy logic-based state-of-health determination of lead acid batteries. In 24th Annual International Telecommunications Energy Conference (pp. 583-590). IEEE.

[59] Singh, P., Fennie Jr, C., & Reisner, D. (2004). Fuzzy logic modelling of state-of-charge and available capacity of nickel/metal hydride batteries. Journal of Power Sources, 136(2), 322-333.

[60] Salkind, A. J., Fennie, C., Singh, P., Atwater, T., & Reisner, D. E. (1999). Determination of state-of-charge and state-of-health of batteries by fuzzy logic methodology. Journal of Power sources, 80(1-2), 293-300.

[61] Anton, J. C. A., Nieto, P. J. G., Viejo, C. B., & Vilán, J. A. V. (2013). Support vector machines used to estimate the battery state of charge. IEEE Transactions on power electronics, 28(12), 5919-5926.

[62] Jun, B. I., WANG, Y. X., & ZHAO, X. M. (2017). State of charge estimation for electric vehicle batteries based on a particle filter algorithm. DEStech Transactions on Computer Science and Engineering, (smce).

[63] Li, B., Peng, K., & Li, G. (2018). State-of-charge estimation for lithium-ion battery using the Gauss-Hermite particle filter technique. Journal of Renewable and Sustainable Energy, 10(1), 014105.

[64] Xia, B., Sun, Z., Zhang, R., & Lao, Z. (2017). A cubature particle filter algorithm to estimate the state of the charge of lithium-ion batteries based on a second-order equivalent circuit model. Energies, 10(4), 457.

[65] Xia, B., Sun, Z., Zhang, R., Cui, D., Lao, Z., Wang, W., ... & Wang, M. (2017). A comparative study of three improved algorithms based on particle filter algorithms in soc estimation of lithium ion batteries. Energies, 10(8), 1149.

[66] Farrokhabadi, M., König, S., Cañizares, C. A., Bhattacharya, K., & Leibfried, T. (2017). Battery energy storage system models for microgrid stability analysis and dynamic simulation. IEEE Transactions on Power Systems, 33(2), 2301-2312.

[67] Thale, S. S., Wandhare, R. G., & Agarwal, V. (2014). A novel reconfigurable microgrid architecture with renewable energy sources and storage. IEEE Transactions on Industry Applications, 51(2), 1805-1816.

[68] Farrokhabadi, M., König, S., Cañizares, C. A., Bhattacharya, K., & Leibfried, T. (2017). Battery energy storage system models for microgrid stability analysis and dynamic simulation. IEEE Transactions on Power Systems, 33(2), 2301-2312.

[69] Van den Bossche, P., Omar, N., Al Sakka, M., Samba, A., Gualous, H., & Van Mierlo, J. (2014). The challenge of PHEV battery design and the opportunities of electrothermal modeling. In Lithium-Ion Batteries (pp. 249-271). Elsevier.

[70] Tang, X., Gao, F., Zou, C., Yao, K., Hu, W., & Wik, T. (2019). Load-responsive model switching estimation for state of charge of lithium-ion batteries. Applied energy, 238, 423-434.

[71] Xu, J., Li, S., & Cao, B. (2017). A novel current disturbance estimation method for battery management systems in electric vehicle. Energy Procedia, 105, 2837-2842.

[72] Ciortea, F., Rusu, C., Nemes, M., & Gatea, C. (2017, May). Extended Kalman Filter for state-of-charge estimation in electric vehicles battery packs. In 2017 International Conference on Optimization of Electrical and Electronic Equipment (OPTIM) & 2017 Intl Aegean Conference on Electrical Machines and Power Electronics (ACEMP) (pp. 611-616). IEEE.

[73] Perez, H. E., Siegel, J. B., Lin, X., Stefanopoulou, A. G., Ding, Y., & Castanier, M. P. (2013, September). Parameterization and validation of an integrated electro-thermal cylindrical lfp battery model. In ASME 2012 5th Annual Dynamic Systems and Control Conference joint with the JSME 2012 11th Motion and Vibration Conference (pp. 41-50). American Society of Mechanical Engineers Digital Collection.

[74] Lin, X., Fu, H., Perez, H. E., Siege, J. B., Stefanopoulou, A. G., Ding, Y., & Castanier, M. P. (2013). Parameterization and observability analysis of scalable battery clusters for onboard thermal management. Oil & Gas Science and Technology–Revue d'IFP Energies nouvelles, 68(1), 165-178.

[75] Lin, X., Perez, H. E., Siegel, J. B., Stefanopoulou, A. G., Li, Y., Anderson, R. D., ... & Castanier, M. P. (2012). Online parameterization of lumped thermal dynamics in cylindrical lithium ion batteries for core temperature estimation and health monitoring. IEEE Transactions on Control Systems Technology, 21(5), 1745-1755.

[76] Hannan, M. A., Hoque, M. M., Hussain, A., Yusof, Y., & Ker, P. J. (2018). State-of-the-art and energy management system of lithium-ion batteries in electric vehicle applications: Issues and recommendations. Ieee Access, 6, 19362-19378

[77] Lu, L., Han, X., Li, J., Hua, J., & Ouyang, M. (2013). A review on the key issues for lithium-ion battery management in electric vehicles. Journal of power sources, 226, 272-288.

[78] Liu, H., Wei, Z., He, W., & Zhao, J. (2017). Thermal issues about Li-ion batteries and recent progress in battery thermal management systems: A review. Energy conversion and management, 150, 304-330.

## APPENDIX A- Equivalent Circuit Parameters

### $R_0$ (Discgarge)

| Tc (°C) / SOC | 5 | 15 | 25 | 35 | 45 |
|---|---|---|---|---|---|
| 0.1 | 0.0190 | 0.0136 | 0.0106 | 0.0090 | 0.0084 |

| | | | | | |
|---|---|---|---|---|---|
| 0.2 | 0.0184 | 0.0134 | 0.0104 | 0.0088 | 0.0082 |
| 0.3 | 0.0182 | 0.0134 | 0.0104 | 0.0090 | 0.0082 |
| 0.4 | 0.0184 | 0.0134 | 0.0104 | 0.0090 | 0.0082 |
| 0.5 | 0.0188 | 0.0136 | 0.0106 | 0.0088 | 0.0082 |
| 0.6 | 0.0190 | 0.0136 | 0.0106 | 0.0086 | 0.0082 |
| 0.7 | 0.0194 | 0.0136 | 0.0104 | 0.0086 | 0.0080 |
| 0.8 | 0.0192 | 0.0136 | 0.0102 | 0.0086 | 0.0080 |
| 0.9 | 0.0194 | 0.0136 | 0.0102 | 0.0086 | 0.0080 |

**$R_0$ (Charge)**

| Tc (℃) / SOC | 5 | 15 | 25 | 35 | 45 |
|---|---|---|---|---|---|
| 0.1 | 0.0166 | 0.0128 | 0.0100 | 0.0088 | 0.0082 |
| 0.2 | 0.0162 | 0.0126 | 0.0100 | 0.0088 | 0.0082 |
| 0.3 | 0.0161 | 0.0124 | 0.0100 | 0.0088 | 0.0082 |
| 0.4 | 0.0160 | 0.0124 | 0.0100 | 0.0088 | 0.0082 |
| 0.5 | 0.0160 | 0.0126 | 0.0100 | 0.0088 | 0.0082 |
| 0.6 | 0.0161 | 0.0126 | 0.0090 | 0.0088 | 0.0082 |
| 0.7 | 0.0164 | 0.0127 | 0.0090 | 0.0088 | 0.0082 |
| 0.8 | 0.0166 | 0.0127 | 0.0090 | 0.0088 | 0.0082 |
| 0.9 | 0.0168 | 0.0126 | 0.0090 | 0.0088 | 0.0082 |

**$R_1$ (Discharge)**

| Tc (℃) / SOC | 5 | 15 | 25 | 35 | 45 |
|---|---|---|---|---|---|
| 0.1 | 0.0500 | 0.0280 | 0.0180 | 0.0130 | 0.0110 |
| 0.2 | 0.0420 | 0.0250 | 0.0170 | 0.0120 | 0.0100 |

| | | | | | |
|---|---|---|---|---|---|
| 0.3 | 0.0360 | 0.0230 | 0.0160 | 0.0110 | 0.0090 |
| 0.4 | 0.0350 | 0.0240 | 0.0190 | 0.0130 | 0.0110 |
| 0.5 | 0.0330 | 0.0230 | 0.0170 | 0.0120 | 0.0100 |
| 0.6 | 0.0300 | 0.0200 | 0.0140 | 0.0100 | 0.0080 |
| 0.7 | 0.0280 | 0.0180 | 0.0130 | 0.0100 | 0.0080 |
| 0.8 | 0.0270 | 0.0190 | 0.0150 | 0.0130 | 0.0110 |
| 0.9 | 0.0260 | 0.0200 | 0.0160 | 0.0110 | 0.0090 |

**$R_1$ (Charge)**

| Tc (℃) / SOC | 5 | 15 | 25 | 35 | 45 |
|---|---|---|---|---|---|
| 0.1 | 0.0230 | 0.0160 | 0.0110 | 0.0090 | 0.0070 |
| 0.2 | 0.0230 | 0.0170 | 0.0120 | 0.0100 | 0.0080 |
| 0.3 | 0.0240 | 0.0180 | 0.0130 | 0.0110 | 0.0090 |
| 0.4 | 0.0240 | 0.0190 | 0.0140 | 0.0120 | 0.0100 |
| 0.5 | 0.0260 | 0.0210 | 0.0160 | 0.0160 | 0.0110 |
| 0.6 | 0.0270 | 0.0220 | 0.0150 | 0.0150 | 0.0100 |
| 0.7 | 0.0280 | 0.0220 | 0.0180 | 0.0150 | 0.0090 |
| 0.8 | 0.0340 | 0.0240 | 0.0180 | 0.0170 | 0.0110 |
| 0.9 | 0.0440 | 0.0490 | 0.0280 | 0.0270 | 0.0130 |

**$R_2$ (Discharge)**

| Tc (℃) / SOC | 5 | 15 | 25 | 35 | 45 |
|---|---|---|---|---|---|
| 0.1 | 0.1000 | 0.0750 | 0.0600 | 0.0500 | 0.0400 |

| | | | | | |
|---|---|---|---|---|---|
| 0.2 | 0.0400 | 0.0390 | 0.0229 | 0.0171 | 0.0171 |
| 0.3 | 0.0380 | 0.0243 | 0.0186 | 0.0129 | 0.0080 |
| 0.4 | 0.0658 | 0.0328 | 0.0229 | 0.0114 | 0.0080 |
| 0.5 | 0.0357 | 0.0243 | 0.0157 | 0.0100 | 0.0080 |
| 0.6 | 0.0300 | 0.0200 | 0.0143 | 0.0080 | 0.0171 |
| 0.7 | 0.0400 | 0.0414 | 0.0229 | 0.0171 | 0.0171 |
| 0.8 | 0.0729 | 0.0429 | 0.0271 | 0.0157 | 0.0170 |
| 0.9 | 0.0400 | 0.0243 | 0.0157 | 0.0100 | 0.0080 |

**$R_2$ (Charge)**

| Tc (℃) / SOC | 5 | 15 | 25 | 35 | 45 |
|---|---|---|---|---|---|
| 0.1 | 0.0243 | 0.0171 | 0.0171 | 0.0129 | 0.0129 |
| 0.2 | 0.0243 | 0.0186 | 0.0186 | 0.0157 | 0.0143 |
| 0.3 | 0.0243 | 0.0200 | 0.0157 | 0.0143 | 0.0114 |
| 0.4 | 0.0329 | 0.0243 | 0.0186 | 0.0114 | 0.0080 |
| 0.5 | 0.0343 | 0.0229 | 0.0186 | 0.0129 | 0.0080 |
| 0.6 | 0.0343 | 0.0200 | 0.0186 | 0.0143 | 0.0114 |
| 0.7 | 0.0300 | 0.0229 | 0.0171 | 0.0114 | 0.0114 |
| 0.8 | 0.0429 | 0.0300 | 0.0214 | 0.0157 | 0.0170 |
| 0.9 | 0.0450 | 0.0643 | 0.0386 | 0.0300 | 0.0157 |

**$C_1$ (Discharge)**

| Tc (℃) / SOC | 5 | 15 | 25 | 35 | 45 |
|---|---|---|---|---|---|
| 0.1 | 1700 | 1900 | 2200 | 2500 | 3000 |
| 0.2 | 1850 | 2050 | 2300 | 2600 | 2900 |
| 0.3 | 1700 | 2100 | 2400 | 2700 | 2900 |
| 0.4 | 1850 | 2150 | 2300 | 2500 | 2750 |
| 0.5 | 1800 | 2200 | 2500 | 2750 | 2850 |
| 0.6 | 1700 | 2150 | 2500 | 2800 | 3100 |
| 0.7 | 1450 | 1850 | 2400 | 2750 | 3300 |
| 0.8 | 1100 | 1600 | 2100 | 2650 | 3100 |
| 0.9 | 900 | 800 | 1600 | 2100 | 3000 |

**$C_1$ (Charge)**

| Tc (℃) / SOC | 5 | 15 | 25 | 35 | 45 |
|---|---|---|---|---|---|
| 0.1 | 800 | 1300 | 1900 | 2400 | 2900 |
| 0.2 | 1000 | 1500 | 1900 | 2200 | 2600 |
| 0.3 | 1300 | 1800 | 2100 | 2500 | 2700 |
| 0.4 | 1500 | 2100 | 2500 | 2850 | 2900 |
| 0.5 | 1600 | 2000 | 2200 | 2500 | 2450 |
| 0.6 | 1700 | 1900 | 2300 | 2650 | 2900 |
| 0.7 | 1800 | 2250 | 2700 | 3300 | 3500 |
| 0.8 | 1900 | 2500 | 3300 | 3700 | 3800 |
| 0.9 | 2000 | 2500 | 2800 | 2800 | 2800 |

**$C_2$ (Discharge)**

| Tc (℃) / SOC | 5 | 15 | 25 | 35 | 45 |
|---|---|---|---|---|---|
| 0.1 | 15789 | 31579 | 36842 | 39474 | 34211 |
| 0.2 | 31579 | 50000 | 65789 | 84211 | 100000 |
| 0.3 | 28947 | 44737 | 73684 | 100000 | 121053 |
| 0.4 | 21053 | 31579 | 39474 | 76316 | 134211 |
| 0.5 | 26316 | 44737 | 71053, | 105263 | 134211 |
| 0.6 | 42105 | 63158 | 86842 | 123684 | 144737 |
| 0.7 | 39474 | 36842 | 47368 | 47368 | 60526 |
| 0.8 | 23684 | 31579 | 36842 | 55263 | 76316 |
| 0.9 | 26316 | 39474 | 65789 | 92105 | 115789 |

**$C_2$ (Charge)**

| Tc (℃) / SOC | 5 | 15 | 25 | 35 | 45 |
|---|---|---|---|---|---|
| 0.1 | 52632 | 60526 | 71053 | 92105 | 84211 |
| 0.2 | 52632 | 73684 | 89474 | 105263 | 121053 |
| 0.3 | 50000 | 68421 | 84211 | 105263 | 110526 |
| 0.4 | 36842 | 47368 | 39474 | 76316 | 134211 |
| 0.5 | 31579 | 44737 | 57895 | 81579 | 134211 |
| 0.6 | 31579 | 55263 | 73684 | 100000 | 110526 |
| 0.7 | 36842 | 50000 | 73684 | 105263 | 121053 |
| 0.8 | 26316 | 34211 | 47368 | 63158 | 86842 |
| 0.9 | 15789 | 28942 | 34211 | 92105 | 60526 |

$O_{cv}$

| Tc (°C) / SOC | 5 | 15 | 25 | 35 | 45 |
|---|---|---|---|---|---|
| 0.1 | 3.2378 | 3.2111 | 3.1714 | 3.1714 | 3.1714 |
| 0.2 | 3.2622 | 3.2444 | 3.2333 | 3.2311 | 3.2311 |
| 0.3 | 3.2733 | 3.2711 | 3.2622 | 3.2600 | 3.2600 |
| 0.4 | 3.2778 | 3.2822 | 3.2822 | 3.2844 | 3.2867 |
| 0.5 | 3.3000 | 3.3000 | 3.3000 | 3.3000 | 3.3000 |
| 0.6 | 3.3000 | 3.3000 | 3.3000 | 3.3000 | 3.3000 |
| 0.7 | 3.3429 | 3.3429 | 3.3429 | 3.3429 | 3.3429 |
| 0.8 | 3.3429 | 3.3429 | 3.3429 | 3.3429 | 3.3429 |
| 0.9 | 3.5000 | 3.5714 | 3.5714 | 3.5429 | 3.5429 |

## **APPENDIX** B- **MATLAB code for Energy Management Criteria**

```
function [I_batref,solar_current,wind_current,load_current]  = fcn(P_pv, P_w, P_L,
SOC, Ts)
delta_P = (P_pv+ P_w) - P_L;
P_max = 24000;
solar_current= P_pv/220;
wind_current= P_w/220;
load_current= P_L/220;
if (Ts>60)
   I_batref=0;
else
   if ((delta_P)<=0) % load is higher than generation
      if (SOC >0.3)
         if((-delta_P)> P_max)
            I_batref= (-P_max)/220;%24000%220
            %state=1;
         else
            I_batref=(delta_P)/220;
            %%state=2;
         end
      else
         I_batref=0;
         %state=3;
      end
```

```
    else
        if (SOC<0.9)
            if ((delta_P)> P_max)
                I_batref= (P_max/220);
                %state=5;
            else
                I_batref= (delta_P)/220;
                %state=6;
            end
        else
            I_batref=0;
            %state=7;
        end
    end
end
```